Journal of Building Engineering 68 (2023) 106068

Contents lists available at ScienceDirect

Journal of Building Engineering

journal homepage: www.elsevier.com/locate/jobe

Simulation of thermal comfort and energy demand in buildings of sub-Himalayan eastern India - Impact of climate change at mid (2050) and distant (2080) future

Samar Thapa [a,*], Hom Bahadur Rijal [b], Wilmer Pasut [a,c], Ramkishore Singh [d], Madhavi Indraganti [e], Ajay Kumar Bansal [f], Goutam Kumar Panda [g]

[a] Department of Environmental Sciences, Informatics and Statistics, Ca' Foscari University of Venice, Mestre, VE, Italy
[b] Faculty of Environmental Studies, Tokyo City University, Japan
[c] Department of Architecture, Korea University, Seoul, South Korea
[d] Lovely Professional University, Phagwara, India
[e] Architecture and Urban Planning Department, Qatar University, Doha, Qatar
[f] School of Engineering and Technology, Central University of Haryana, India
[g] Department of Electrical Engineering, Jalpaiguri Government Engineering College, WB, India

ARTICLE INFO

Keywords:
Climate change
Thermal comfort
Heating degree day
Cooling degree day
Overheating
Under-cooling

ABSTRACT

The global warming associated with climate change predicted by the Intergovernmental Panel on Climate Change (IPCC) is expected to deteriorate the indoor climate of free-running buildings. Features like proper orientation and wall thickness are important for the design of a building that is resilient to the impact of climate change. However, the implementation of these features is sometimes difficult, especially in a rugged hilly location. A whole building simulation was performed using DesignBuilder for an existing 3-storey free running multi-family concrete building located in the sub-Himalayan region of eastern India, for thermal comfort and energy demand during the present and the climate change scenarios of 2050 and 2080. The results show an increasing trend in the indoor operative temperature during the future climatic scenario, with the condition inside the top roof-exposed floor deteriorating the most. A decrease of 59.8% and 81.2% in the annual heating energy and an increase of 221.9% and 467.0% in the annual cooling energy were predicted for the future climate of 2050 and 2080 compared to the present. Parametric analysis performed considering orientation, wall U-value, infiltration rate and window-to-wall ratios revealed that the east/south-east facing orientation would perform the best with regard to overheating due to climate change. Further, the use of autoclaved aerated concrete (AAC) brick is recommended along with the decrease in air infiltration rate and window-to-wall ratio to improve the thermal performance of the indoor environment. In addition, we have also proposed a method to assess the under-cooling of an indoor environment.

1. Introduction

A large portion of time is spent indoors by a modern human being. The indoor environment thus needs to be comfortable and healthy. As a result, the thermal comfort of the indoor environment is one of the most studied topics even after over 50 years of

* Corresponding author.
E-mail addresses: samar_thapa2005@yahoo.co.in, samar.thapa@unive.it (S. Thapa).

https://doi.org/10.1016/j.jobe.2023.106068
Received 12 November 2022; Received in revised form 28 January 2023; Accepted 5 February 2023
Available online 11 February 2023

research [1]. Though, the American Society of Heating, Refrigerating and Air-Conditioning Engineers, ASHRAE Standard 55 [2] provides a relatively simple definition of thermal comfort as "that condition of mind which expresses satisfaction with the thermal environment", thermal discomforts of indoor environment are still the most commonly expressed dissatisfactions inside a building [3]. Two methods are commonly used for the evaluation of thermal comfort, first, the climate chamber based predicted mean vote – predicted percentage of dissatisfaction (PMV – PPD) developed by Fanger [4] in the early seventies, and second, the adaptive model of thermal comfort which was also first proposed in the seventies by Nicol et al. [1] and later recommended by de Dear and Brager [5]. These methods which provide the guidelines for indoor comfort conditions also help to optimse the energy use in buildings. This is essential as over 40% of the energy used worldwide contributes to the building sector for its construction, operation and maintenance [6]. This implies that a reduction of energy consumption in this sector even by a small fraction can lead to substantial savings in a country like India having a huge population. This is in-fact essential considering the recent call by the IPCC vide its Sixth Assessment Report (2022) for an urgent and drastic reduction in the global anthropogenic carbon dioxide (CO_2) emissions (50% by 2030 and net zero by 2050) in order to limit the global warming by 1.5 °C [7].

A major portion of the energy used inside buildings is dedicated to providing a comfortable indoor environment, primarily using the HVAC (heating, ventilating and air conditioning) utilities. Regarding the use of air conditioning in buildings to provide a thermally comfortable environment, Haves et al. [8] stated that the energy used and thus wasted, acts as a significant driver of global warming, creating a positive feedback loop, as higher ambient temperature ultimately leads to greater use of air conditioners altogether. Whether it was the extraordinarily hot summer of 2003 [9] or the extreme heat wave in 2022 in Europe, experts have warned that the rate of global warming is faster than previously envisaged in any of the worst-case scenarios [9]. Difficulties for the existing buildings are anticipated by the progressively and more frequent extreme climate events. More than 35,000 people died in Europe during the heat wave of the summer of 2003 [10]. Hayhoe et al. [11] estimated a seven-time increase in the death rate due to high temperatures in Los Angeles despite acclimatization by the year 2090. Studies have suggested that deadly heatwaves could occur for as much as 60 days annually in the mid-latitude region of the world and this has the potential to affect 48–74% of the world's population by the end of this century [12]. Overheating-related mortality and morbidity are seen in different parts of the world. However, due to the adaptation of human beings, the threshold temperatures are different and are higher in the cooling-dominated regions [13]. Even India witnesses an increasing trend in death due to heat waves [14]. The sub-Himalayan region of eastern India, where the present study is located usually experiences a monthly mean temperature of 15.5 °C during the month of June [15], which is calculated over a period of 30 years. This region experienced a maximum recorded temperature of 28.1 °C on 25th June 2019 which is considered 3.1 °C above the normal [16].

India, which is projected to become the third largest emitter of carbon dioxide after the US and China by 2030 [17] is also expected to warm by 0.5 °C by the same time from the present [18]. Problems like an increase in the heat waves, frequency of extreme weather events, and changes in the monsoon and precipitation pattern which affect the agricultural productivity and melting of glaciers, thus causing water crises are highly anticipated. Additionally, due to the loss of productivity and submergence of coastal areas, climate-induced migration would be a major problem causing the cities to be more crowded and putting enormous pressure on the socio-economic structure as more houses need to be built. Reports suggest that 75% of the buildings that will exist in India by 2030 are yet to be built [19].

Studies have revealed that the present buildings or those constructed with the present standards could become increasingly difficult to operate and maintain during future climatic conditions [20]. Li et al. [21] state that naturally ventilated buildings are more vulnerable to the risk of overheating. Yang et al. [22] found a more significant increase in the cooling demand than a decrease in the heating demand in the Nordic countries. The study conducted with three batches of climatic data for the period 2010–2039, 2040–2069, and 2070–2099 for the residential building stocks in 38 European cities over five different climatic zones revealed an increase in the cooling demand in the future across all cities, and the frequency and intensity of the heat waves and extreme warm hours increased considerably by the end of the present century [22]. Most of the studies conclude that in the next few decades, the cooling energy demand will far exceed the heating energy demand [23]. An increase in peak electricity demand by 0.5–4.6% is predicted for every degree of temperature rise [24].

Different studies have tried to use different methods to quantify the overheating of the indoor environment. Apart from the Chartered Institution of Building Services Engineers, CIBSE TM 52 [25], which prescribes the commonly known steady-state model of overheating criteria, Hamdy et al. [26] introduced the concept of indoor overheating hours (IOH), indoor overheating degree (IOD) and ambient warmness degree (AWD). These are discussed in section 2.3.1 below. Rahif et al. [27] recently introduced the concept of Climate Change Overheating Resistivity (CCOR) as the rate of change of IOD with the increasing AWD. They further found that the Variable Refrigerant Flow (VRF) with Dedicated Outdoor Air Supply (DOAS) was more effective in reducing the indoor operative temperature compared to the Variable Air Volume (VAV) for the climate change scenarios in the cities of New Delhi, Cairo, Buenos Aires, Brussels, Toronto and Stockholm. Zou et al. [28] simulated the outdoor extreme heat events and indoor overheating for a residential representative building for the three Canadian cities of Montreal, Toronto and Vancouver for the three climatic scenarios of (i) 2001–2020 (contemporary); (ii) 2041–2060 (near term future); and (iii) 2081–2100 (long term future), respectively. They found that extreme warm year (EWY) and extreme cool year (ECY) efficiently captured the maximum and the minimum monthly overheating hours and provided the upper and lower boundary of the indoor and outdoor most probable overheating conditions.

In India too, studies on thermal comfort of indoor environment have gained interest in recent years. However, considering the Indian sub-continent which is diverse both climatologically and culturally, these studies are sporadic and those in the cold climatic regions are few [29, 30]. Needless to say that the simulation based studies are even rarer in these climatic regions. Using the Trsnsient System Simulation Tool, TRNSYS for the vernacular buildings at three different bioclimatic zones in north-east India, Singh et al. [31] found that none of the selected houses were significantly comfortable in winter and summer months as per the International Organization for Standardization, ISO 7730. Heena et al. [32] used EnergyPlus DesignBuilder to study the performance of vernacular

houses in the future climate of 2030, 2040 and 2050 in the cold climate of Bishoi in western Himalayas. However, with the rapid urbanization and construction of concrete structured buildings, the vernacular architecture is less common. Also, it is anticipated that the modern concrete buildings which are 'framed' having post and beam have a longer lifetime than the vernacular architecture which has 'load bearing' walls.

Though, the Indian building standards like the National Building Code [33] and Energy Conservation Building Code [34] provides the recommendatory guidelines, it is well understood that the use of solar passive features is beneficial to both thermal comfort and energy conservation especially in cold climate [35]. Proper orientation is one of the most important criteria of a solar passive building. The south-facing buildings in the northern hemisphere and the north-facing ones in the southern hemisphere are observed to have the most comfortable indoor environment and are also the most energy efficient. In this regard, Hamdy et al. [26] had predicted a 15.2% lesser discomfort in buildings that are oriented towards the south/north than those oriented towards east/west direction and are also more resilient towards climate change. Escamilla et al. [36] predicted a 25% more hours of thermal comfort per year with the use of double skin on the south façade of a building in the city of Santiago de Cali. However this desired orientation of buildings is often limited to external factors, like landscape in a rugged location, or congestion in urban setting, etc. In hilly regions, where the buildings are located along the slope of the hill, the choice for proper orientation for a building is not available. Several other studies focused on the overheating of indoor environment due to the climate change [37, 38 and 39]. However, studies elaborating the performance of buildings especially in the face of climate change in such a rugged hilly location are scarce, especially in the Himalayan region of India which experiences a cold climate. Needless to say that these regions are also highly vulnerable towards the effect of climate change [17].

Unlike the Energy Efficiency Directive of the European Commission [40] which makes it compulsory for the newer buildings to be nearly Zero Energy Buildings (nZEB) or atleast class A (energy efficient) buildings, there are no such mandatory legislations for buildings built in a developing country like India. Further, the launch of 'Pradhan Mantri Awas Yojana' in 2015 which is a flagship government programme to provide housing to the urban poor in the next decade by constructing over 20 million affordable housing has led to a rapid growth in construction of residential buildings [41]. Though at present, most of the residential houses in India are of free-running type, this is expected to change with the increased economic status and expectation from indoor thermal and visual environment, thus causing a rise in the use of air conditioning (AC) equipments in the coming decades. The figure could further be sky-rocketed due to the expected climate change and the global warming. India which still relies for over 70% of its power generation on fossil fuel resources, the rise in the use of ACs can easily raise the CO_2 emission and thus increase the global warming. Previous studies have shown that the impact of climate change is more rapid and extreme in the temperate regions than the tropical ones.

In this study, we examine the whole building performance of a multi-family, concrete 3-storey building built on the west-facing hill slope of Darjeeling Himalayan region in eastern India. The effects due to global warming on the future climatic scenarios of 2050 and 2080 are extrapolated. The objective of this research is to study the thermal performance of a representative existing building in the face of climate change. The study also aims to estimate the change in the energy demand for heating and cooling in order to provide a comfortable indoor condition. The parametric evaluation of wall U-values, orientation, ventilation rate and window-to-wall ratios will enable designers or architects in the region or in regions elsewhere with similar geo-climatic set up to evaluate trade-offs between these different factors and construct buildings that are more resilient in the face of climate change. We also propose a method to assess the under-cooling of the indoor environment as the investigated building is located in a cold climate region in India. Further, unlike the previous studies which considered only the indoor air or operative temperature to study the effect of climate change, the studied locations being situated in the humid region of India, we have considered both indoor operative temperature and relative humidity by representing them in the psychrometric charts and compared it with the comfortable region recommended by ASHRAE standard 55 [2] and thermal comfort field study in the region.

2. Methodology

2.1. Model generation

In order to assess the indoor environment of concrete buildings being built in the lower Himalayan region of eastern India, an existing building was modeled using the whole building simulation tool DesignBuilder version 6 which uses the EnergyPlus simulation engine. The idf (input data file) editor in EnergyPlus provides a platform to generate the building model. However, the building optimization tool DesignBuilder, which uses EnergyPlus for simulation provides a graphical interface to create and visualize the model.

The tool, EnergyPlus is however sensitive to user inputs, whose results often cause uncertainty among the modelers [42]. Ioannou and Itard [43] have predicted that the input-led discrepancies could increase from 30 to 100% from the actual energy performance in energy performance simulations (EPS). Hosseini et al. [44] state that the hourly results obtained by EPS can be calibrated with the measured hourly values, which can eliminate the effects caused due to uncertainties, reduce discrepancies in the measured profiles, and have a realistic indoor environmental assessment. Thus, the validation of the outputs was done using the measured indoor air temperature. The indoor monitoring was done at a frequency interval of every 10 min from 8th to 17th November 2021, using temperature sensors hygrometers. These sensors were placed on top of a table away from any direct source of radiation.

The model constructed in DesignBuilder was simulated for the indoor environmental parameters like indoor operative temperature, relative humidity, etc. during the present climatic scenario and for the climate change conditions of the year 2050 and 2080, respectively. These indoor operative temperatures obtained from the whole building simulation were analyzed for indoor thermal comfort as discussed in section 2.3 below. Additionally, simulations were also conducted for the heating and cooling energy demands in the present and future scenario, should the building be conditioned. Fig. 1 illustrates the proposed methodology.

Further, in order to evaluate the parametric differences, separate simulations were conducted with the validated model for each

variation in orientations, envelope wall U-value, rate of infiltration, and window-to-wall ratios.

2.2. Climatic conditions and projection for future scenarios

The IPCC based on factors like demographic change, economic development, and technological changes extrapolates the future condition by the year 2100 into 4 divergent groups [45].

- A1 scenario: This describes the future world having rapid economic growth along with the population that peaks around the mid of the century and thereafter declines. They are also based on economies that include the rapid introduction of new and more efficient technologies.
- A2 scenario: This scenario describes that of heterogeneous culture, which is representative of continually increasing population and economic development that are regionally oriented.
- B1 scenario: This represents the population that peaks in the middle of the century and declines thereafter as in the A1 scenario. However, in this setting with an increase in the use of clean and resource-efficient technologies, the stress on natural resources decreases.
- B2 scenario: This represents a rapidly growing population as in A2, however, the economic development is lesser compared to that in A2.

It is acknowledged that the effects of climate change are global and not just isolated. However, considering the heterogeneity of economy and culture in different regions, IPCC states that there is a high uncertainty due to the driving forces of emissions on climate modeling and assessment of impacts, vulnerability, mitigation, etc. [45]. The A2 scenario of the IPCC was selected in this study, which predicts a high carbon dioxide emission by the end of 21st century along with fast and continued population growth and a swift rise in the economy, as seen in countries like China and India. The second most important criterion for selecting the A2 scenario is the fact that it considers the net positive anthropogenic CO_2 emissions related to change in the land use pattern (as seen from rapid urbanization, etc.) and increasing economic growth. This is in contrast to the B1 scenario, in which case the emission of CO_2 declines fast. The typical meteorological year (TMY) weather data of nearby Taplejung airport (in Nepal) was taken from the epw (EnergyPlus Weather) files. Morphing of the present meteorological conditions as per the projected trends of the General Circulation Model (GCM) was done using the tool CCWorldWeatherGen ® V 1.9 (2017), which uses the HadCM3 prepared by the Hadley Centre for Climate Prediction and Research as the GCM. Fig. 2 shows the daily outdoor temperature of the current and the climate change scenarios of 2050 and 2080 for the studied location.

2.3. Metrics

2.3.1. Overheating criteria

There are several ways of assessing the discomfort caused by indoor overheating apart from the traditional metrics of degree hours (above the base temperature of 18 °C). The CIBSE Guide A for Environmental design [25] prescribes the commonly known steady-state model of overheating criteria. It states that for the living rooms, the operative temperature should not increase over 28 °C for more than 1% of the occupied hours. The same for the bedrooms is restricted to 26 °C for over 1% of occupied hours.

However, the steady-state criteria do not consider the adaptation (climatic) made by the occupants with the change in outdoor temperature or the way the building is used. Thus, as a revised form, the CIBSE Technical Memorandum, TM 52 [46] proposed the risk of overheating in naturally ventilated buildings based on the thermal comfort criteria set by the European Standard EN 15251 [47], now superseded by EN16798 [48]. Risk of overheating is considered if any two of the three following criteria are not met by the indoor condition.

- Criterion 1 (Hours of exceedance, h_e): This first criterion sets a limit to the number of hours that the operative temperature can exceed the threshold comfort temperature. It states, that the operative temperature (T_{op}) should not exceed the maximum

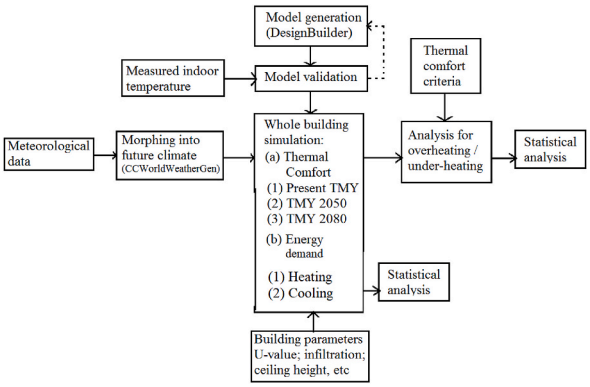

Fig. 1. Workflow of the proposed method.

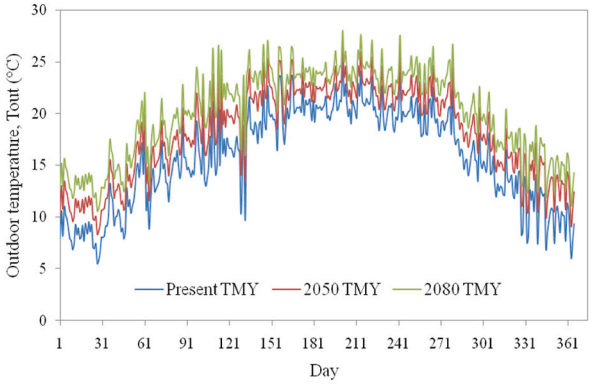

Fig. 2. Daily outdoor temperature variation (in °C) during the present and future scenarios in the studied location.

temperature (T_{max}) by 1 °C or higher for over 3% of the occupied hours. T_{max} is the upper threshold temperature as per the adaptive standards set by EN15251 [47] for category II limits (i.e., the Predicted Percentage of Dissatisfied <10%) and given in eq. (1).

$$T_{max} = 0.33T_{rm} + 21.8 \tag{1}$$

Where, T_{rm} is the running mean of outdoor air temperature for the day.

- Criterion 2 (Daily weighted exceedance, W_e): This criterion assesses the daily severity of overheating, i.e., both in temperature rise and in duration over time. The weighted exceedance, W_e (in eq. (2)) should be lesser than 6 degree-hours for any given day.

$$W_e = \sum h_e \times w_f \tag{2}$$

Where h_e is the number of hours of exceedance and w_f is the weighting factor, given by

$$w_f = \begin{cases} 0 \text{ if } T_{op} < T_{max} \\ T_{op} - T_{max}, \text{otherwise} \end{cases} \tag{3}$$

- Criterion 3 (Upper limit temperature, T_{upp}): This criterion sets a limit to the maximum indoor temperature (i.e. the T_{op} shall not exceed the T_{max} beyond 4 °C) for the room, above which the overheating is unacceptable and the usual adaptive measures are insufficient to restore thermal comfort.

Furthermore, the more recently published Technical Memorandum TM 59 [49] lays a stricter criterion for bedrooms, i.e., the steady-state condition for bedrooms laid by CIBSE Guide A [25] plus the Criterion 1 (i.e., hours of exceedance, h_e) laid by TM 52 [46], respectively.

2.3.2. *Under-heating*

In addition to the indoor overheating caused due to the apprehended global warming as per IPCC [50], under-heating of the indoor environment is highly prevalent in the region of the present study. This is mostly due to the insufficient insulation thickness owing to either because of economic reasons or climatic conditions as the buildings in the region experience high humidity (indoor RH during summer: 53 – 91%) [51], which needs further investigation.

The World Health Organization (WHO) prescribes a temperature range of 18–24 °C for sedentary activities in the indoor environment [52]. Though the standard ASHRAE 55 prescribes a lower temperature of 18 °C for 90% acceptability limits, the CIBSE TM 52 [46] doesn't provide guidelines for calculating the under-heated environment. Although, the heating degree day (HDD) provides an indirect method to determine the energy needed to heat a space from below the base temperature, a direct method to evaluate the under-heated environment is highly sought.

In accordance with the indoor overheating hours (IOH) of Hamdy et al. [26], we hereby propose a direct method to calculate the indoor under-cooled hours (IUC). Eq. (4) below returns the annual total number of hours in zone 'z', for which the indoor operative temperature, T_{op} is below the lower limit of the comfort temperature, T_{L_comf}.

$$IUC = \sum_{i=1}^{N_z} \text{undercooling} \times t_{i,z} \tag{4}$$

where,

$$\text{undercooling} = \begin{cases} 1, \text{when } \left(T_{L\_comf,i,z} - T_{op,i,z}\right) > 0 \\ 0, \text{otherwise} \end{cases} \tag{5}$$

In the above equations, (4)–(5), 'i' is the occupied hour; 'N_z' is the total occupied hours in zone 'z'; and 't' is the time step of 1 h. The lower limit of comfort temperature, T_{L_comf} is calculated from the adaptive thermal comfort equations (eq. (6)) of Thapa et al. [51] based on field investigation in the same region with a sample size of 2608 in the year 2015. For living rooms, the ASHRAE Standard 55 [2] prescribed lower 80% acceptance limit (T_{comf} – 3.5 °C) is considered, while for the bedrooms where the adaptation opportunities employed by the subjects are limited, a stricter ASHRAE Standard 55 [2] lower 90% acceptance (T_{comf} – 2.5 °C) criteria are used.

$$T_{L\_comf} = 0.593T_{rm} + 10.18, R = 0.796, N\ 2608, p < 0.001 \tag{6}$$

The IOH [26] and the IUC only give the annual number of hours during which the indoor environmental condition is above or below the established comfort limits. For assessing the intensity of overcooling, the indoor under-cooling degree (ICD) is proposed in accordance with the indoor overheating degree (IOD) of Hamdy et al. [26]. The ICD as illustrated in eq. (7) below represents the severity of indoor overcooling by taking into consideration of both the temperature difference and the time of occupancy.

$$ICD = \sum_{i=1}^{N_z} \left[\min\left\{T_{L\_comf,i,z} - T_{op,i,z}, 0\right\} \times t_{i,z}\right] \Big/ \sum_{i=1}^{N_z} t_{i,z} \tag{7}$$

2.3.2.1. Ambient warmness degree. The severity of outdoor warmness is measured as the ambient warmness degree (AWD), which is the average cooling degree day (CDD) hours calculated with a T_b (base temperature) of 18 °C [26]. Hamdy et al. [26] state that the $CDD_{18\ ^\circ C}$ for the summer months should be used for the calculation of $AWD_{18\ ^\circ C}$. This value of base temperature as 18 °C for AWD (eq. (8)) is further validated by the work of Bhatnagar et al. [53] from their study in different cities of India.

$$AWD_{18^\circ C} = \frac{\sum_{i=1}^{N} \max\left\{T_{a,i} - T_b, 0\right\} \times t_i}{\sum_{i=1}^{N} t_{i,z}} \tag{8}$$

In the above equation (8), $T_{a,i}$ represents the ambient air temperature at the ith time step and N is the number of hours during which the ambient air temperature is over the base temperature ($T_{a,i} \geq T_b$), respectively.

2.4. Simulation

The EnergyPlus Version 8 in the DesignBuilder (version 6.3) was used to simulate the indoor condition for the present TMY and the future climatic scenarios of 2050 TMY and 2080 TMY, respectively. The TMY 2050 and TMY 2080 represent the mid-future and distant future [28] for climate change modeling within the century [45]. A more distant future is considered in the present study compared to the previous work of Heena et al. [32] which considered up till 2050 only. This is because the studied building which is made up of concrete having beams and pillars is expected to have a longer life than that of the vernacular buildings in Heena et al. [32] which usually have load-bearing walls. The simulation result contains 17 zones in the three floors of the building for 8760 hours resulting in 178,760 data points for each climatic scenario. Zoning of the buildings was done as default by the software which uses the planimetry of the building.

3. Case study

As stated above (in section 1), the construction of concrete houses is on the rise with the economic growth of Indian society. However, due to the terrain, most of the houses in the hilly region are of low to mid-rise (i.e. below 15 m in height), housing up to a few families in the same building. Thus, an existing 3 storey multi-family building which is representative of the buildings built in the sub-Himalayan region in Darjeeling and other similar regions in India was modeled. This was done using the whole building simulation tool DesignBuilder version 6 which uses the EnergyPlus simulation engine. The building is situated in the geographical coordinates, 26.88° N latitude, 88.28° E longitude having an elevation of 1420 m above the mean sea level (MSL). The region lies in the lower Himalayan areas in eastern India, where there are several hill stations, like Darjeeling, Kurseong, Kalimpong, Shillong, etc. which have experienced urbanization since the British era in India favored due to its temperate type of climate [54]. The weather classification of the region falls under cold climate as per the National Building Code (NBC) of India [33] and as sub-tropical highland oceanic climate (Cwb) with reference to the Koppen climate type.

The building was constructed in the year 2004 and has its longer orientation along north-south (west facing). However, due to the non-mandatory nature of building codes in India, no insulations are present. The top exposed roof of the building is made from

Table 1
Thermal and other properties used in the simulation of the modeled building (SGHC: solar heat gain coefficient).

Sl. No.	Component	Thickness (Dimension)	U-value ($W/m^2.K$)	Thermal capacitance ($kJ/m^2.K$)
1	Envelope wall (brick)	0.1250 m	3.102	128.73
2	Partition wall (brick)	0.1250 m	2.425	128.73
3	External Roof (tinned)	0.0060 m	3.261	3.50
4	Internal Floor (concrete slab)	0.1266 m	2.896	229.53
5	Ground Floor (concrete)	0.1125 m	3.166	193.48
6	Window (single glazing) window to wall ratio: 30%	SHGC: 0.699	5.942	Solar transmission: 0.603
7	Infiltration	5.00 air change per hour (ACH)		
8	Occupancy	0.02 people/m^2		

galvanized iron sheet having a gradient of 25°. A false ceiling made up of plywood measuring 0.8 cm is present below the roof with an air gap of 10 cm. The inter-partition floor is made up of 10 cm RCC (reinforced cement concrete) slab with 1.25 cm cement plaster on both sides. The envelope is made up of 12 cm fire clay brick with 1.5 cm cement plaster on both sides. The building envelope values were obtained from the building plan which is provided in a previously published paper, Thapa [55]. The final thermal properties of the different elements of the modeled building are illustrated in Table 1. The studied building being a residential one, the occupancy schedule for the different rooms/zones were measured by the first author himself and shown in Table 2.

In the hilly and rugged location, where the modeled building exists, landscape is a more important factor than the neighboring buildings causing obstruction of sunlight. The present modeled building is constructed on the west facing hill slope of the range, as a result, substantial obstruction of solar radiation occurs on the eastern wall. In fact, the building's eastern wall is below grade up till the mid of the first floor, thereby increasing the ground contact and thermal capacitance. Fig. 3 (a) show the floor plan of the first floor while Fig. 3 (b) and (c) shows the west (front) face and the north face of the modeled building, respectively.

3.1. Description of the projected climate scenarios

The analysis of the present and future climate scenarios is discussed in this section. It was seen that the outdoor air temperature increase in the future climate scenarios as predicted by the IPCC [50]. Fig. 4 is a psychrometric chart showing the distribution of outdoor air temperature during the present and the climate change scenarios of 2050 and 2080 for the region, respectively. An increasing trend in the outdoor air temperature during the future climate conditions was noticed. The outdoor air temperature ranged between 0.3 and 35.0 °C, 5.0–35.6 °C and 7.9–36.0 °C in the summer months (March–October) and between 0.6 and 21.0 °C, 3.8–22.6 °C, and 6.0–24.9 °C in the winter months (November–February), during the climatic conditions of the present, 2050 and 2080 respectively. Table 3 shows the seasonal mean outdoor air temperature. A mean value of 18.3 °C (s d. 4.4 °C), 20.6 °C (s d. 4.0 °C) and 22.5 °C (s d. 3.9 °C) in the summer months and 10.6 °C (s d. 4.2 °C), 13.2 °C (s d. 3.9 °C) and 15.2 °C (s d. 3.9 °C) in the winter months for the present TMY, 2050 and 2080 was noticed. This difference in mean hourly outdoor air temperature between different climatic years was statistically significant, Friedman's 2-way ANOVA, χ^2 (N = 8760, d. f. = 2): 17520.0, $p < 0.001$. Thus, there was an increase in mean temperature by 2.4 °C in the year 2050 and 4.3 °C in the year 2080. However, the increase in the mean outdoor temperature was observed to be more (by 2.6 °C in 2050 and 4.6 °C in 2080) during the winter months (Nov–Feb) than (by 2.3 °C in 2050 and 4.2 °C in 2080) summer months (Mar–Oct), respectively. A reason for the higher increase in the ambient temperature during the winter months could be due to the lesser RH during these months (Table 3), which otherwise acts as a reservoir of heat source/sink. This is in accordance with the previous work of Dino and Akgul [56] who had found that the increase in temperature due to climate change would be more prominent during the cool season than during the warm season. Other previous studies also have shown an increase in annual mean temperature by 1.8–2.9 °C for the various Mediterranean locations [57] and up to 2 °C during the winter months in southern Spain in the future climate scenarios of 2050 compared to the present. Fig. 5 shows the percentage distribution of the hourly outdoor air temperature under different climatic scenarios. The findings reflect that in future climatic conditions, higher outdoor air temperatures become more common in this elevated Himalayan region, which is presently classified as a cold climate region. It is noticed that the frequency of hourly temperatures above 20 °C tends to increase whereas that below 20 °C decrease in the future climatic conditions compared to the present. The highest increase in temperature frequency, 9.9% in the range of 20–25 °C was seen to occur between the present condition and that in 2050, followed by 9.1% in the range of 25–30 °C between the year 2050 and 2080, respectively. The severity of outdoor warmness is measured by the AWD which is the amount of CDD normalized with the time during the warmer season. The AWD values were 3.2 K, 4.1 K and 5.2 K for the present, 2050 and 2080 climatic conditions, respectively. Dino and Akgul [56] report AWD of 3.5 K and 6.4 K for the baseline and year 2060 for Istanbul.

The mean relative humidity decreased slightly in the future climate conditions, i.e., 77.5% (s.d. 16.1%), 77.0% (s.d. 16.1%) and 75.6% (s.d. 16.7%) during the present, 2050 and 2080 climatic conditions. The difference was statistically significant, χ^2 (df = 2): 7773.7, $p < 0.001$. Also, the mean global horizontal radiation decreased slightly in the future climate conditions, i.e., 204.4 W/m^2 (s d. 286.5 W/m^2), 197.5 W/m^2 (s d. 277.0 W/m^2) and 195.6 W/m^2 (s d. 274.5 W/m^2) during the present, 2050 and 2080 climatic conditions. This difference was also statistically significant, χ^2 (df = 2): 6465.34, $p < 0.001$.

The monthly HDD and CDD are shown in Fig. 6, while their annual values are shown in Table 3. The amount of increase in the annual CDD was comparable to the decrease in the annual HDD between the future and the present climatic condition. The annual HDD decreased by 504 °C-days (43.2%) and by 790 °C-days (67.6%), while the annual CDD increased by 370 °C-days (106.0%) and by 788 °C-days (225.8%) during the climatic condition of 2050 and 2080, compared to the present climate, respectively. A previous study by Dino and Akgul [56] has shown similar results in the decrease of HDD by 27.2%, 20.7%, 13.8% and 10.3%, while an increase in CDD by 90.9%, 157.2%, 176.4% and 150.9% in the cities of Izmir, Istanbul, Ankara and Erzurum during 2060 than the baseline year.

Table 2
Details of occupancy and schedule for simulation (refer: Fig. 3 (a)).

Zone wise occupancy			Schedule (percentage occupancy)			
Sl No	Zone (Refer Fig. 3 (a))	Occupancy (people/m^2)	Time (hr)	Bedroom	Kitchen	Living Room
1	Toilet	0.0196	22–6	1.0	0	0
2	Bedroom 1	0.0260	6–8	0.4	0.6	0
3	Living Room	0.0220	8–14	0	0.4	0.6
4	Kitchen	0.0900	14–18	0.2	0.4	0.4
5	Bedroom 2	0.0870	18–22	0	0.8	0.2

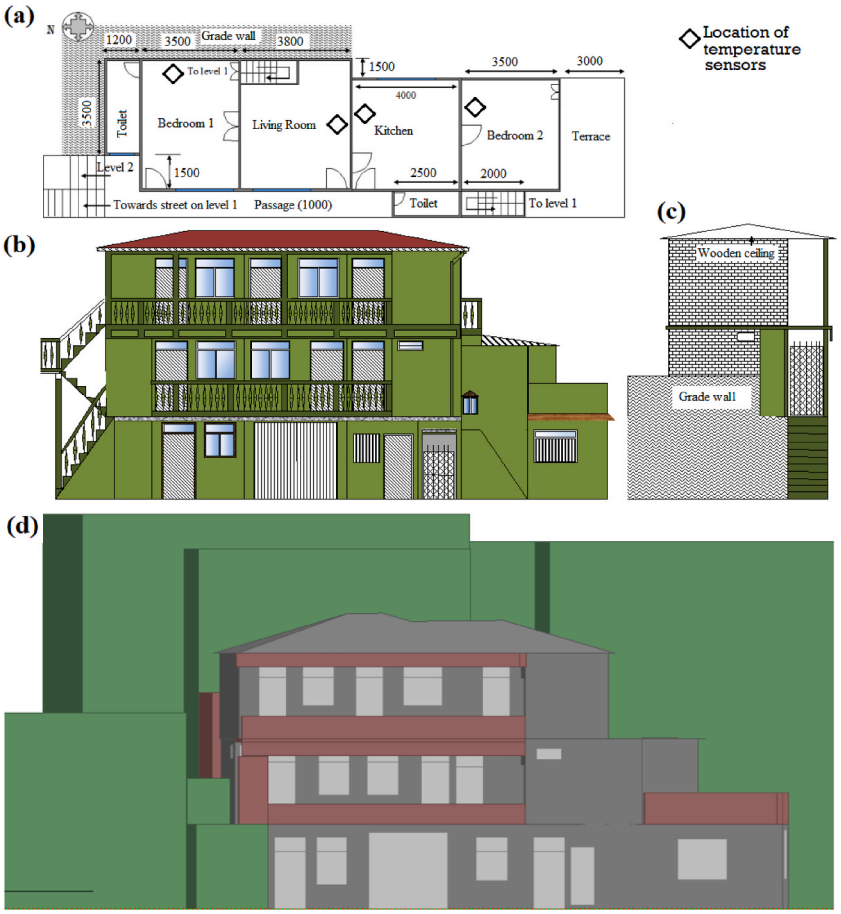

Fig. 3. (a) Floor plan of the first floor of the modeled building (note: the east and north wall is below grade till the middle); (b) west section (front face) of the building; (c) north face of the building showing the grade wall; and (d) model of the building in DesignBuilder. The green background in (d) represents the hill slope on the eastern side (back) of the building (Ref: Thapa [55]). (For interpretation of the references to color in this figure legend, the reader is referred to the Web version of this article.)

3.2. Validation of the model

In order to have reliable outputs from the building simulation models, measured data were used to validate the simulated data for the monitoring period. The measurements were done using a temperature hygrometer and a data logger at a frequency of 10 min. The device with the trade name Hero's Digital hygrometer having a range of −10 °C to +50 °C and an accuracy of ±0.1 °C for air temperature and a range of 0–100% with an accuracy of ±1% for relative humidity was used to monitor the indoor environmental conditions. The hygrometer sensors were positioned away from the direct source of radiation (like windows), at a height supported on a table in each of the bedrooms and living rooms (shown in Fig. 3 (a)). The measurements were done during the autumn season, i.e., from the 8th to the 17th of November 2021, with an aim to grasp the variation caused due to changing outdoor conditions. The outdoor environmental conditions of air temperature, dew point temperature, relative humidity, air velocity and solar radiation were taken from the World Weather Online server, which provides the historical weather data of the location under study every 15 min intervals. The outdoor data from 1 month prior to the beginning of the date of indoor temperature measurements were substituted in the epw file for running a simulation of the built model for its validation. It is however acknowledged by the authors that the calibration of the model for one full year is done with an on-site measurement of environmental parameters for only 10 days, which is low considering the factors like seasonal variations. However, previous studies in the region [51] have suggested that due to the high relative humidity experienced over the entire year, a higher day–night variation is observed rather than the seasonal variation.

Fig. 7 (a) shows the measured and simulated indoor air temperature. The coefficient of variation of the root mean square error, i.e., CV(RMSE) and the normalized mean bias error (NMBE) are two statistical methods recognized by international standards [58] for measuring the validity of the energy models.

$$\mathrm{CV(RMSE)} = 100 \times \frac{1}{\bar{y}} \sqrt{\left[\sum_{i=1}^{n} \frac{(y_i - \hat{y}_i)^2}{n}\right]} \tag{9}$$

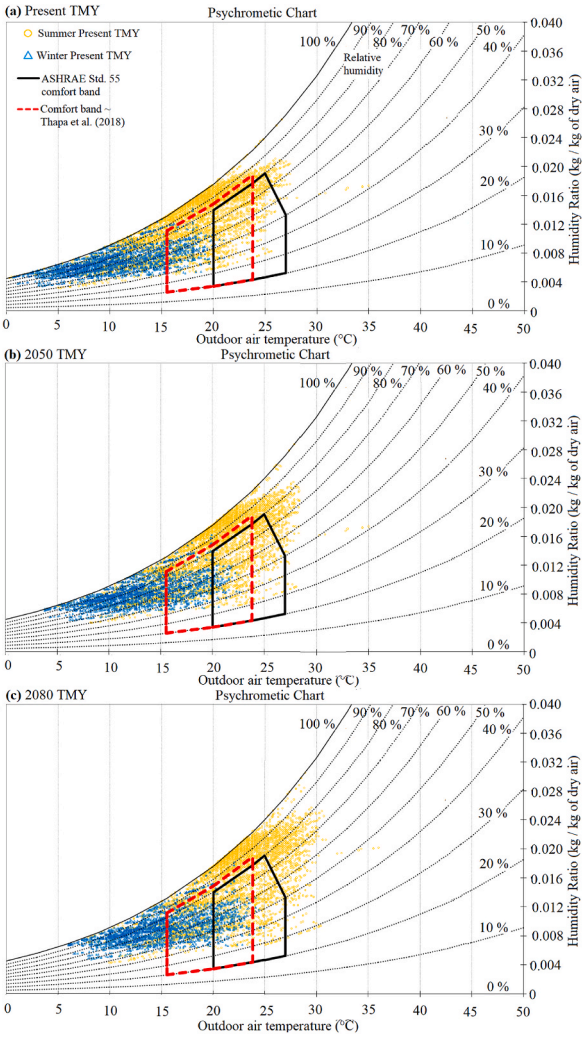

Fig. 4. Distribution of outdoor air temperature during the (a) present TMY; (b) TMY 2050; and (c) TMY 2080 climatic conditions.

Table 3
Statistics of outdoor temperature (T_{out}) and relative humidity (RH) during the present and the climate change scenarios (TMY: typical meteorological year; HDD: heating degree day (K-days); CDD: cooling degree days (K-days); AWD: ambient warmness degree (K); W: winter; S: summer; and Y: yearly).

		Present TMY			2050 TMY			2080 TMY		
		W	S	Y	W	S	Y	W	S	Y
T_{out} (°C)	Mean	10.6	18.3	15.8	13.2	20.6	18.2	15.2	22.5	20.1
	s.d.	4.2	4.4	5.6	3.9	4.0	5.3	3.9	3.9	5.2
Annual warmness	HDD	1168 K-days			664 K-days			378 K-days		
	CDD	349 K-days			719 K-days			1137 K-days		
	AWD	3.2 K			4.1 K			5.2 K		
RH	Mean	73.5	79.4	77.5	73.5	78.7	77.0	71.7	77.6	75.6
	s.d.	14.3	16.6	16.1	14.1	16.8	16.1	14.1	17.6	16.7
Global horizontal radiation (Wh/m^2)	Mean	163	225	204	160	216	197	160	213	196
	s.d.	241.8	304.0	286.5	237.0	292.9	277.0	236.9	289.5	274.5

$$NMBE = 100 \times \frac{\sum_{i=1}^{n}(y_i - \hat{y}_i)}{n.\bar{y}} \quad (10)$$

In the above equations 9 and 10, $\hat{y}_i$ stands for simulated value at the time 'i', y_i is the measured hourly value at the time 'i' and $\bar{y}$ is the mean of the measured value. NMBE cancels out the negative and the positive values and thus tends to eliminate the bias, whereas the CV(RMSE) does not cancel this bias. Though the model calibration was done by adjusting the U-value and the infiltration rate, no

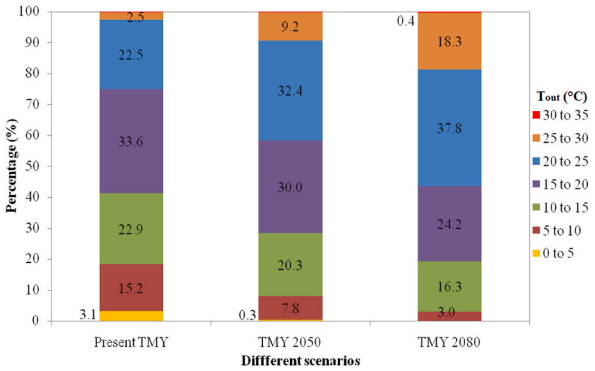

Fig. 5. Percentage distribution of the hourly outdoor temperature, T_{out} (°C) under different climatic scenarios.

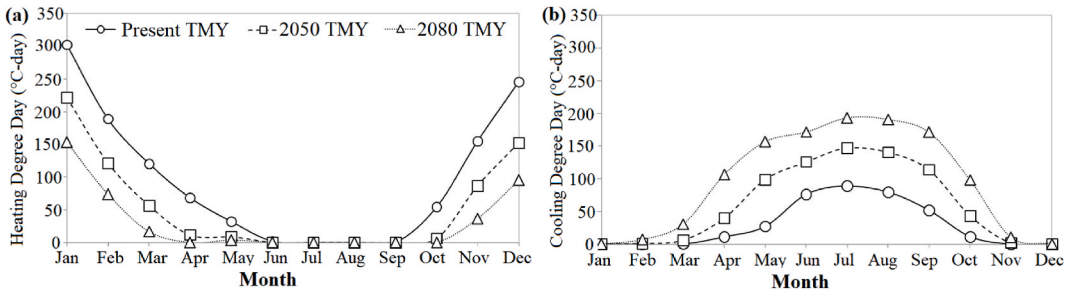

Fig. 6. (a) Monthly heating degree day (HDD) and (b) cooling degree day (CDD) for the different climatic scenarios (base temperature 18 °C).

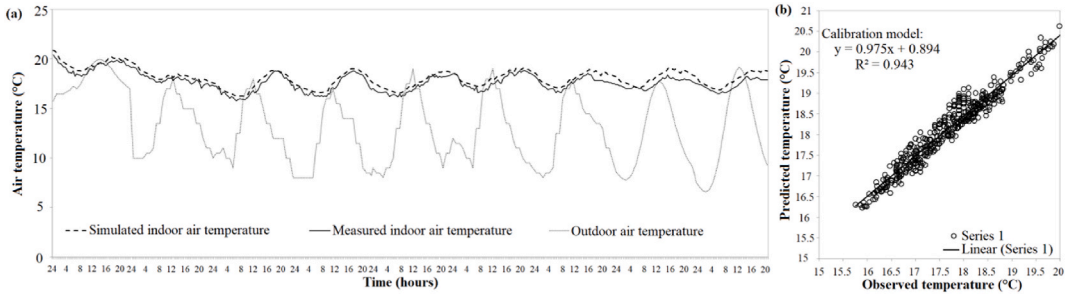

Fig. 7. (a) Indoor and outdoor air temperature during the measured period; and (b) calibration of the model.

blower door tests were done for the spaces to adjust the infiltration rates. However, the rates of infiltration were taken from the recommended values of NBC [33] for NV buildings in India. A CV(RMSE) value of 3.99% and NMBE value of 3.11% were noticed for the present model, which was well within the recommended value of lesser than |±10%|. Also, the predicted model showed a strong correlation ($R^2 = 0.89$) with the observed model (Fig. 7 (b)).

4. Results

4.1. Assessment of indoor environment

The indoor operative temperature (T_{op}) and the relative humidity (RH) from each zone were segregated as per the floors and as per the vertical section. Fig. 8 illustrates these points in the psychrometric chart, which also shows the comfort band as prescribed by the ASHRAE Standard 55 [2] and the comfort band obtained from the field survey study comprising 2608 sample size in the same location by Thapa et al. [59]. The shifting of the data points towards the right in the future climatic scenario represents the warming of the indoor environment. Though the T_{op} points currently falling left of the ASHRAE Standard 55 [2] comfort band at present TMY in Fig. 8 (a) and (d) which represents the under-cooled indoor environment, gets shifted towards the right in Fig. 8 (b - c) and (e - f), thereby falling within the boundaries of the comfortable region, those points currently within the boundaries of the comfortable region gets further shifted towards right. In addition, the points which are above the comfort band represent a high RH. This causes a hot and humid conditions causing discomfort. The extension of the lower limit in comfort temperature obtained from Thapa et al. [59] shown

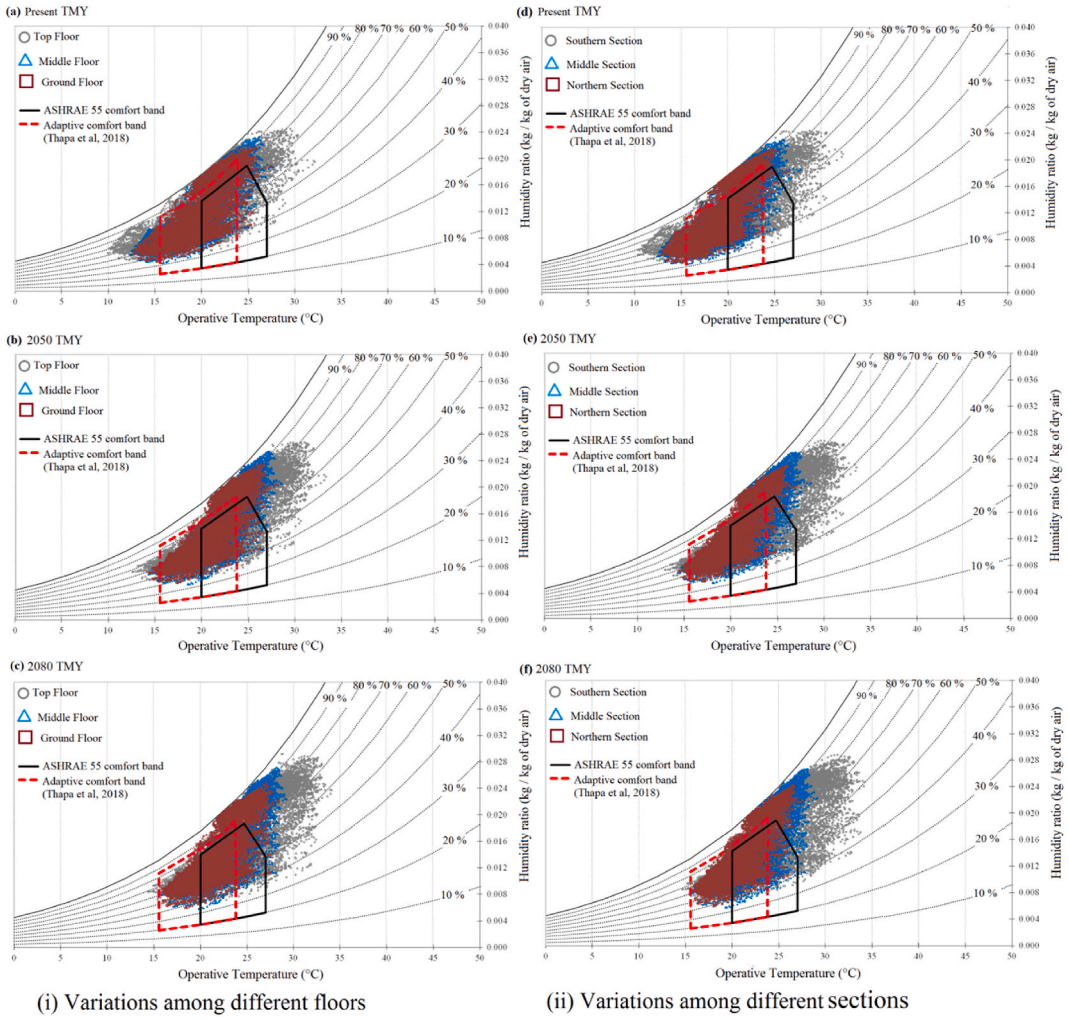

Fig. 8. Variation of indoor conditions (operative temperature and relative humidity) in the (i) left - different floors (grey circles: top floor; blue triangles: middle floor; and brown squares: ground floor) and (ii) right - in different sections (grey circles: southern; blue triangles: middle; and brown squares: northern) during the different climatic conditions (a) & (d) present TMY; (b) & (e) 2050 TMY; and (c) & (f) 2080 TMY. The bounded surface by black solid lines indicate the ASHRAE Standard 55 comfort zones and that by red dashed lines the adaptive comfort zone based on the field study of Thapa et al. [30] which was conducted in the same region. (For interpretation of the references to color in this figure legend, the reader is referred to the Web version of this article.)

in Fig. 8 is based on the field study in different buildings in the same region. However, the authors acknowledge that with the changing climatic conditions and with the consequent adaptations acquired by the residents this limit is subject to change.

Fig. 9 illustrates the floor-wise and vertical section-wise variation in the percentage of indoor operative temperature. It was interesting to note that in the present condition, 39.8%, 42.1% and 49.7% of the time the T_{op} were below 20 °C, while for 5.9%, 0.1% and 0% of the time they were above 27 °C in the top, middle and ground floor. During the 2050 climatic conditions, 22.3%, 24.8% and 31.2% of the time the T_{op} were below 20 °C, while 22.4%, 1.4% and 0.1% of the time were above 27 °C in the top, middle and ground floor. Similarly, in the 2080 climatic condition, an estimated 13.5%, 16.6% and 21.8% of the time the T_{op} were below 20 °C, while for 37.6%, 7.8% and 0.9% of the time they were above 27 °C in the top, middle and ground floor, respectively. These results show an increasing trend in indoor operative temperature in the future climatic condition, as evident from the increase in the percentage of the period for which the indoor operative temperature is above 27 °C and a decrease in the percentage of the period for which the indoor operative temperature is below 20 °C.

Among the different vertical sections of the building, 35.1%, 44.7% and 56.4% of the time the T_{op} was lesser than 20 °C, while 7.5%, 0.1% and 0.0% of the time T_{op} was over 27 °C in the south, middle and north part in the present climatic condition. During the 2050 climatic conditions, 18.9%, 27.2% and 36.8% of the time, the T_{op} were lesser than 20 °C, while for 24.8%, 0.8% and 0% of the time the T_{op} were over 27 °C in the south, middle and north part of the building, respectively. Similarly, in the 2080 climatic condition, around 11.7%, 18.5% and 26.9% of the time, the T_{op} were lesser than 20 °C, while for 39.3%, 4.8% and 0.1% of the time the T_{op} were over 27 °C in the south, middle and north part in the building, respectively. The results indicate that both during the present and the climate change scenarios of 2050 and 2080, the southern part of the building gets heated above 27 °C for a significant duration.

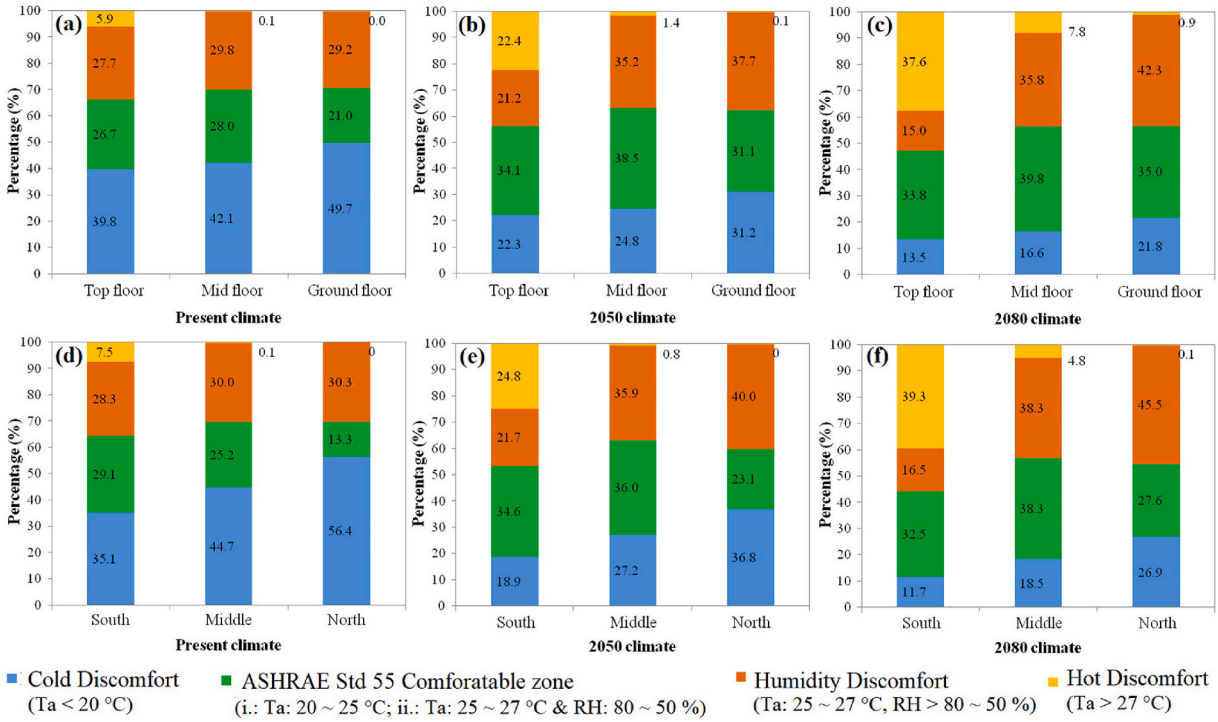

Fig. 9. Percentage distribution of indoor operative temperature during the present and future climate scenarios, (a) ~ (c): floor wise variation; (d) ~ (f): section wise variation.

4.2. *Assessment of overheating/under cooling*

In this section, we discuss the overheating and under-cooling of the indoor environment following the metrics discussed in section 2.3.1 and section 2.3.2.

4.2.1. *Overheating*

The CIBSE TM 52 [46] states an overheated condition if at least 2 out of three conditions are exceeded, i.e., hours of exceedance (h_e), daily weighted exceedance (W_e) and upper-temperature limit (T_{upp}). Fig. 10 illustrates the annual number of overheated days for different zones of the different floors during the present and future climatic years. The average number of overheating days (as per CIBSE TM 52) were 8.5 days (s.d. 7.1 days), 44.5 days (s.d. 25.3 days) and 91 days (s.d. 36.5 days) in the top (roof exposed) floor, followed by 2.1 days (s.d. 4.4 days), 11.7 days (s.d. 18.9 days) and 24.7 days (s.d. 37.5 days) in the first (middle) level and 5.7 days (s.d. 13.4 days), 14.8 days (s.d. 35.9 days) and 22.3 days (s.d. 53.3 days) in the ground floor during the present, 2050 and 2080 climatic conditions, respectively. A previous study has shown 47% lesser indoor overheating hours on non-roof-exposed floors than on roof-exposed floors [54]. This suggests that the mid floors are the least overheated during the present and the climate change scenarios of 2050, whereas as expected the top (roof exposed) floor returns the most overheated conditions in all three climates. It is further noticed that overheating days occur in all rooms of the top (roof exposed) floor, with a significant increase inside the rooms situated along the southern and western parts. In contrast, on the lower (non-roof-exposed) floors, i.e., the first floor and the ground floor, only the rooms situated on the southern side exhibit overheating both during the present and the future climatic years.

4.2.2. *Under-cooling*

The indoor under-cooling (IUC) hour is the annual number of hours for which the operative temperature is below the 80%

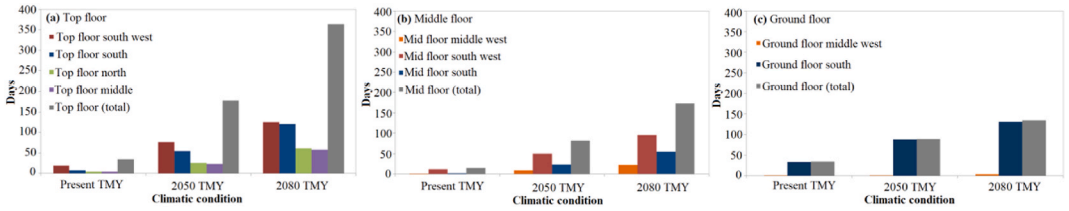

Fig. 10. CIBSE overheating assessment (in days annually) of overheating during the present, 2050 and 2080 climatic conditions (a) top floor; (b) middle floor; and (c) ground floor.

acceptability of the comfort temperature for the day. The annual IUC for the different floors under different climatic conditions is illustrated in Fig. 11. The floor-wise mean annual number of IUC were 332 h, 25 h and 7 h on the top floor, 194 h, 33 h and 16 h on the mid floor and 306 h, 246 h and 56 h on the ground floor during the present, TMY 2050 and TMY 2080 scenarios, respectively. A significant decrease in the mean annual number of under-cooling (IUC) hours was noticed in the future climatic conditions, χ^2 (df = 2): 11.7, N = 17, $p < 0.05$ with a mean rank of 2.6, 1.8 and 1.7 between the present, 2050 and 2080 climatic conditions. The numbers of under-cooling hours were most prominent on the ground floor, whereas in the top roof exposed floor it was the least for almost all the climatic conditions. Also, the rooms having walls below the grade (not exposed to the ambient) were less subjected to under-cooling than those rooms having the most exposed surfaces to the ambient.

The number of under-cooling hours (IUC) does not however represent the intensity of under-cooling. The mean indoor under-cooling degree (ICD) was least on the middle floor (Table 4) due to its lesser exposure to the ambient condition. The ICD was highest on the ground floor, which could be due to the fact that it receives the least amount of solar flux. However, the differences in mean ICD between the floor levels or between different climatic scenarios were not statistically significant.

4.3. Assessment of annual heating and cooling energy requirement

Apart from some intermittently used electric or coal-based stoves during some of the extreme winter evenings (Dec–Jan), the building presently runs mostly in free-running mode. However, additional, simulations were performed with the built model under different climatic scenarios with the objective to calculate the energy that would be required for heating and cooling (both normalized to the floor area), using grid-connected electricity. The simulation set point for heating and cooling was set to 18 °C and 26 °C, respectively. The set point temperature for heating is based on the HDD [53], while that for cooling is based on the comfort temperature limit provided by the NBC of India [33]. Fig. 12 shows the monthly variation in the heating and cooling load in kWh/m^2 during the present and future climatic scenarios. A decrease of 59.8% and 81.2% in the annual heating energy requirement and an increase of 221.9% and 467.0% in the annual cooling energy requirement were noticed in the future climate of 2050 and 2080 in comparison to the present condition. A previous study has shown that heating demand decreases by 37% (in Venice) and by 76% (in Palmero) in the year 2065 then the present, while in the same period, the cooling demand increased by 175.5% (in Venice) and by 68.4% (in Palmero), respectively [60].

Fig. 13 shows the floor-wise normalized energy demands for heating and cooling in the present and future climatic scenarios. The heating energy demand (Fig. 13 (a)) exceeded by 329.3%, 701.6% and 1521.2% on the ground floor and by 45.3%, 64.5% and 99.3% on the top floor than that on the middle floor during the present, 2050 and 2080 climatic conditions, respectively. In contrast, the cooling energy demand (Fig. 13 (b)) exceeded by 141.6%, 110.6% and 98.3% on the top floor during the present, 2050 and 2080 climatic conditions, while it exceeded by 23.7% during the present but was lesser by 21.5% and 27.5% during 2050 and 2080 conditions on the ground floor compared to that on the middle floor. However, the decrease in the heating energy demands in the future years was the largest that of 75.3% and 93.7% on the middle floor followed by 72.1% and 91.4% on the top floor and 53.9% and 76.4% on the ground floor during 2050 and 2080 from the present, respectively. Similarly, the increase in the cooling energy demand was highest on the middle floor (292.3% and 625.7%), followed by the top floor (242.0% and 494.5%) and ground floor, (148.9% and 325.6%) during the future climatic scenarios (2050 and 2080) in comparison to that in the present TMY.

Fig. 14 illustrates the vertical section-wise normalized energy demands for heating and cooling in the present and future climatic scenarios. The heating energy demand (Fig. 14 (a)) exceeded by 134.7%, 204.2% and 359.6% in the north part of the building and by 47.9%, 35.8% and 46.0% in the south part of the building than that in the middle section during the present, 2050 and 2080 climatic conditions. Similarly, the cooling energy demand (Fig. 14 (b)) exceeded by 29.9%, 17.3% and 11.7% in the north section and by 642.2%, 499.4% and 424.4% in the southern section of the building than that in the middle section during the present, 2050 and 2080 climatic conditions, respectively. The heating energy demand decreased by 76.1% and 93.6% in the south section, by 74.0% and 93.5% in the middle section and by 66.3% and 87.3% in the northern part during the future climatic conditions of 2050 and 2080 compared to that in the present. Similarly, the cooling energy demand increased by 272.2% and 584.8% in the middle section, 236.2% and 488.8% in the north section and by 200.7% and 383.9% in the southern part of the building during the future climatic conditions of 2050 and 2080 compared to that in the present.

4.4. Parametric differences on the thermal comfort and energy demand

Parametric differences allow estimating the sensitivity of the model in addition to helping us lay the design guidelines. Variations in the orientation of the building, wall U-value, infiltration rate and window-to-wall ratios were studied. These factors are expected to affect the heating and cooling energy demand in both the present and future climatic conditions.

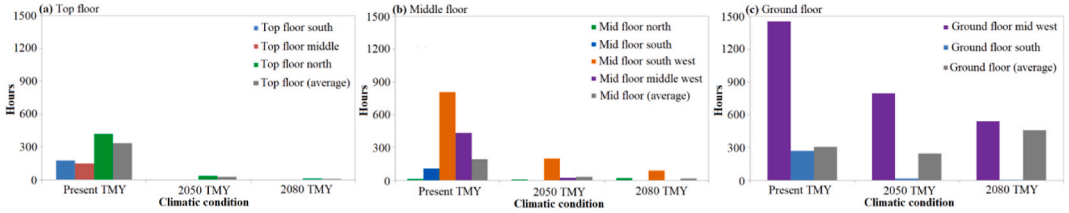

Fig. 11. Number of indoor under cooled hours (IUC) during the present, 2050 and 2080 climatic conditions (a) top floor; (b) middle floor; and (c) ground floor.

Table 4
Indoor under cooling degree (ICD) for the different levels under different climatic scenarios.

Level	Statistics	Climatic scenarios		
		Present	2050	2080
ground floor	mean	0.45	5.02	6.11
	std. Dev.	0.47	5.94	6.31
	N	6	6	6
middle floor	mean	0.38	3.11	2.62
	std. Dev.	0.47	4.31	3.56
	N	7	7	7
top floor	mean	0.75	3.58	2.82
	std. Dev.	0.23	3.80	3.31
	N	4	6	4

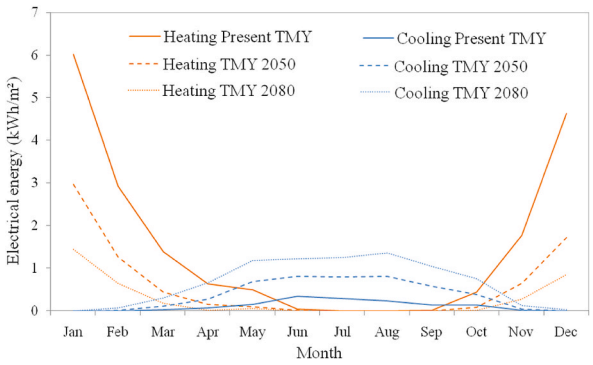

Fig. 12. Monthly heating/cooling (electrical) energy requirement (in kWh/m^2).

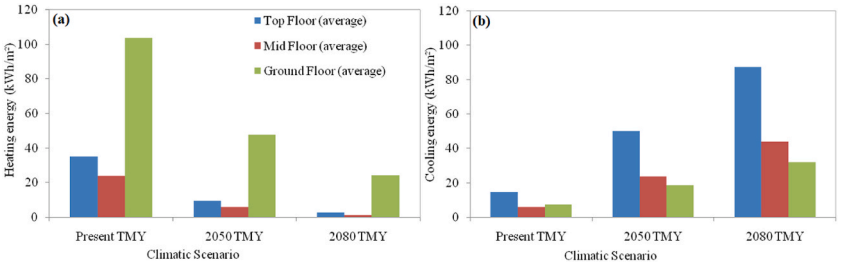

Fig. 13. Floor wise energy demand in different climatic scenarios (a) for heating; and (b) for cooling.

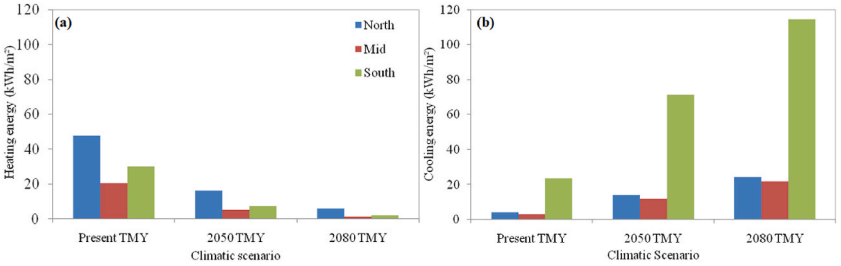

Fig. 14. Vertical section wise energy demand in different climatic scenarios (a) for heating; and (b) for cooling.

4.4.1. Orientation

The investigated building faces due west and has its longer axis along the north-south direction (Fig. 3 (a)). Limitations on the choice of proper orientation are posed by the rugged landscape in a hilly location. This causes a major obstruction on the solar flux apart from the interaction of the building with the more stable (and perhaps cooler) ground. However, the exploration of the effects due to the difference in orientation allows us to estimate the comfort and energy demand for a building located on the other similar

faces of the hill slope having a different direction. Fig. 15 shows the annual variation in the thermal comfort factors of CIBSE overheating days and indoor under-cooled hours and in the energy demand (electrical) for heating and cooling (normalized with the floor area) with the variation in the orientation (facing) of the building, i.e., south (0°), south-west (45°), west (90°), north-west (135°), north (180°), north-east (225°), east (270°) and south-east (315°), respectively.

It is seen from Fig. 15 (a) that the existing orientation (west) of the building is the worst-case scenario as per the CIBSE overheating criteria as it returns 94, 167 and 199 days of indoor overheating during the present, 2050 and 2080 scenarios. Thus, even though the building is located in a cold climatic zone, it is significantly overheated. A similar building facing due south exhibit 40.4%, 36.5% and 25.1% lesser number of overheating days (Table 5) during the present, 2050 and 2080 climatic scenarios, respectively. From Fig. 15 (b) it is noticed that if the same building was located on the east-facing slope it would have been more under-cooled than that from its present orientation by 135%, 396.9% and 614.6% during the present, 2050 and 2080 scenarios, respectively.

Thus, as expected the annual heating energy demand of 1.8, 1.7 and 1.7 kWh/m^2 in the north-east, east and north-facing orientations were higher by 14.6%, 13.6% and 9.1% than that of 1.5 kWh/m^2 in the existing west facing orientation for the present climatic condition. The results were similar for the future climatic scenarios, with north-east, east and north-facing orientations showing 18.2%, 16.5% and 13.1% higher heating energy demands in 2050 and 20.5%, 18.6% and 15.0% higher heating energy demands in 2080, respectively, than that for the existing west facing orientation.

In contrast, the annual cooling energy demands in the south-facing orientation were the lowest, i.e., with 1.6, 6.0 and 11.2 kWh/m^2 were 32.0%, 20.1% and 15.7% lower than the 2.4, 7.6 and 13.3 kWh/m^2 in the west facing orientation during the present, TMY 2050 and TMY 2080 climatic conditions, respectively. However, the rise in the demand for cooling in the future climatic years was the sharpest in the south-facing orientation, i.e., by 278.1% and 602.7% and the least along the north-west orientation, i.e., by 190.4% and 423.8% in the year 2050 and 2080, respectively, in comparison to that in the present (Table 5). This suggests that although at present the orientation facing the west is already overheated, the increase in indoor overheating is more severe in the orientations facing south, which at present is the least overheated. This result is in concurrence with the previous observations of Dino and Akgul [56].

The difference in orientation in a rugged hilly location where the hilly slope acts as an obstruction to the solar radiation causes a considerable difference in solar gain with different orientations of the building. Fig. 16 shows the difference in hourly solar gain with different orientations of the investigated building during the different climatic scenarios. The highest and the lowest mean annual solar gain were observed along the southwest and the northeast direction, 0.65 kWh/m^2 (s.d. 1.22 kWh/m^2, N 8760) versus 0.45 kWh/m^2 (s.d. 0.85 kWh/m^2, N 8760), 0.62 kWh/m^2 (s.d. 0.18 kWh/m^2, N 8760) versus 0.43 kWh/m^2 (s.d. 0.82 kWh/m^2, N 8760) and 0.62 kWh/m^2 (s.d. 1.18 kWh/m^2, N 8760) versus 0.43 kWh/m^2 (s.d. 0.82 kWh/m^2, N 8760) during the present, TMY 2050 and TMY 2080 climatic scenarios, respectively. A decrease in the indoor solar gain with future climatic scenarios was observed in almost all the orientations which are in concurrence with the previous researchers [26], except the south-facing orientation, where there was an increase of 16.0% in the annual solar gain during the climatic scenario of 2080 compared to that in the present.

4.4.2. Wall U-value

It is a fact that thermal envelope renovation actions are increasing all over the world. However, several constraints are imposed on envelope design in this part of the world. The fragile nature of the high altitudinal Himalayan area asks for a lightweight design as seen from several vernacular architectures being made from wood which is mostly of single floor level. However, with the congestion being felt due to urbanization, more concrete and mid-rise buildings are being built. Secondly, the regions being narrow due to steep hill slope offer less floor area, thus envelope with relatively smaller thickness are preferred. Lastly, persistent moisture penetration owing to high outdoor relative humidity throughout the year affects and often degrades the performance of the insulation material used over time, thus requiring further research in the field. Though there is no thermal insulation in the investigated building, neither the NBC

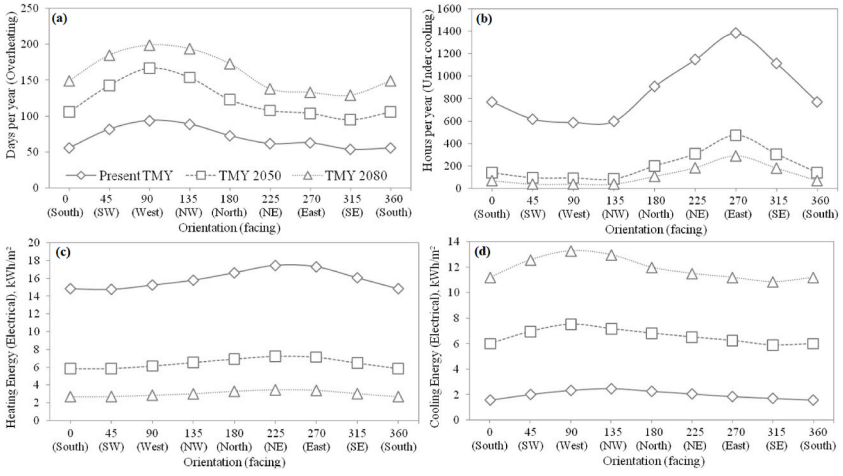

Fig. 15. Variation of (a) CIBSE overheating (days per year); (b) Indoor under cooling hours (hours per year); (c) heating energy demand; and (d) cooling energy demand with different orientation of the building under different climatic scenarios.

Table 5

Percentage change (with respect to the base/existing model (in grey colored rows)) in the annual overheating, under-cooling, heating energy demand and cooling energy demand during the present and future climatic scenarios under various parametric differences (Note: positive values indicate an increase while negative values indicate a decrease).

Parameter	Description of parameters	Value	Change in annual CIBSE Overheating days (in %)			Change in the annual under-cooling (IUC) hours (in %)			Change in the annual heating (Electrical) demand (kWh/m^2) (in %)			Change in the annual cooling (Electrical) demand (kWh/m^2) (in %)		
			Present	TMY 2050	TMY 2080	2050 – Present	2080–2050	2080 – Present	2050 – Present	2080–2050	2080 – Present	2050 – Present	2080–2050	2080 – Present
Orientation (degree)	South	0	−40.4	−36.5	−25.1	31.1	49.0	75.6	−2.7	−4.8	−5.9	−32.0	−20.1	−15.7
	South-West	45	−12.8	−14.4	−7.0	5.1	2.1	0	−3.2	−4.6	−5.5	−13.3	−7.4	−5.4
	West *(base model)*	90	0	0	0	0	0	0	0	0	0	0	0	0
	North-West	135	−5.3	−7.8	−2.5	1.9	−8.3	2.4	3.6	6.5	5.1	5.7	−4.7	−2.4
	North	180	−22.3	−26.3	−13.1	54.5	112.5	168.3	9.1	13.1	15.0	−3.0	−9.3	−9.8
	North-East	225	−34.0	−35.3	−30.7	95.1	224.0	356.1	14.6	18.2	20.5	−11.6	−13.4	−13.4
	East	270	−33.0	−37.7	−33.2	135.0	396.9	614.6	13.6	16.5	18.6	−20.4	−16.9	−15.7
	South-East	315	−42.6	−43.1	−35.2	89.1	221.9	346.3	5.4	5.7	5.8	−26.2	−21.7	−18.3
Wall U-value (W/m^2.°C)	*Existing* single brick layer (0.10 m)	3.1	0	0	0	0	0	0	0	0	0	0	0	0
	Double brick layer (0.25 m)	2.0	−13.8	−13.2	−7.0	−46.3	−83.3	−97.6	−14.1	−14.0	−10.1	−53.8	−32.2	−29.2
	Single AAC brick (0.09 m)	1.0	−22.3	−21.0	−11.6	−73.0	−99.0	−100.0	−27.5	−23.8	−17.2	−53.9	−39.2	−35.6
	Single AAC brick (0.20 m)	0.5	−10.6	−18.0	−10.6	−82.9	−100.0	−100.0	−30.2	−24.0	−17.4	−57.1	−44.7	−40.5
Infiltration (ACH)	Low	2	−12.8	−15.0	−6.0	−9.3	−33.3	−43.9	−2.5	−3.0	−3.2	−6.8	−4.3	−3.9
	High *(existing)*	5	0	0	0	0	0	0	0	0	0	0	0	0
Window-to-wall ratio	Smaller	20	0	−1.4	−0.5	1.3	3.1	0	0.2	0.2	0.2	−3.8	−2.0	−1.5
	Existing model	30	0	0	0	0	0	0	0	0	0	0	0	0
	Bigger	50	3.7	0.7	0.5	−2.4	−4.7	0	−0.2	−0.2	−0.2	9.9	4.8	3.5
	Bigger	80	3.7	2.8	1.1	−5.8	−10.9	0	−0.4	−0.4	−0.3	33.0	16.1	9.6

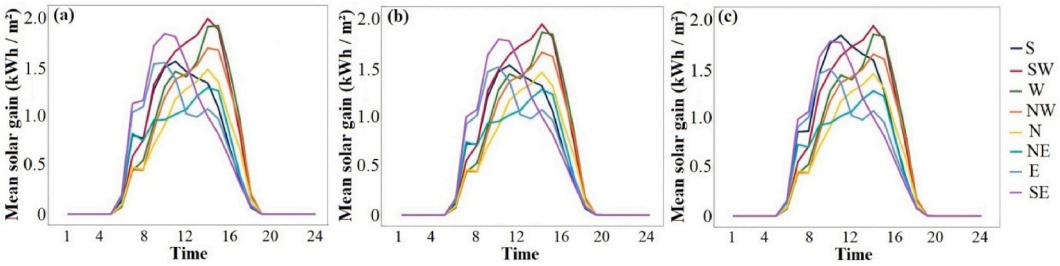

Fig. 16. Hourly solar gain (kWh/m^2) under different orientation during (a) Present TMY; (b) 2050; and (c) 2080.

[33] of India makes a mandatory inclusion of thermal insulation in the built environment, use of alternative designs in the wall façade is common. For example, the use of autoclaved aerated concrete (AAC) brick in place of fire clay brick or the covering of the external façade with the designed clay tiles which are more resistant to weather stresses than the paints is on the rise. Further, the buildings in the region usually have a single layer of brick, i.e., having a wall thickness of about 12–14 cm only, which is mainly for the purpose of making the building light weighted. This suggests that very little consideration is presently given to the thermal performance of the building during its design phase. This leads to the fact that with the increased discomfort due to climatic variation along with the increased economic status and expectation from the thermal environment, an increase in the conditioning of indoor space is highly anticipated in the future.

Four different wall designs were considered, i.e., (i) the existing single fire clay brick (10 cm) layer with 1.25 cm plaster on both sides having U-value (overall heat transfer coefficient) 3.1 W/m^2.°C; (ii) a double layer of fire clay brick with plaster on both sides (total wall thickness 0.25 m) having U-value 2.0 W/m^2.°C; (iii) single AAC bricklayer (total wall thickness 0.09 m) having U-value 1.0 W/m^2.°C; and (iv) double AAC bricklayer (total wall thickness 0.20 m) having U-value 0.5 W/m^2.°C, respectively. It is seen from Fig. 17 (a) that the CIBSE annual overheating days first decrease with the decrease in the wall U-value (increase in thermal insulation) and reaches a minimum value of 73, 132 and 176 days during the present, 2050 and 2080 for wall U value as 1.0 W/m^2.°C, thereafter increases again. Thus, a decrease of U-value from 3.1 to 1.0 W/m^2.°C led to a decrease in indoor overheating days by 22.3%, 21.0% and 11.6% during the climatic conditions of the present, 2050 and 2080, respectively. The slight increase of overheating at a very low U-value is due to the fact that the heat loss from the indoor to the ambient cannot take place effectively, which is in concurrence with previous research [26].

However, with the increase in thermal insulation or the decrease in the wall U-value, there occurred a sharp and clear decrease in the annual indoor under-cooling hours reaching a minimum value (101, 0 and 0 h during the present, 2050 and 2080) at 0.50 W/m^2.°C, respectively.

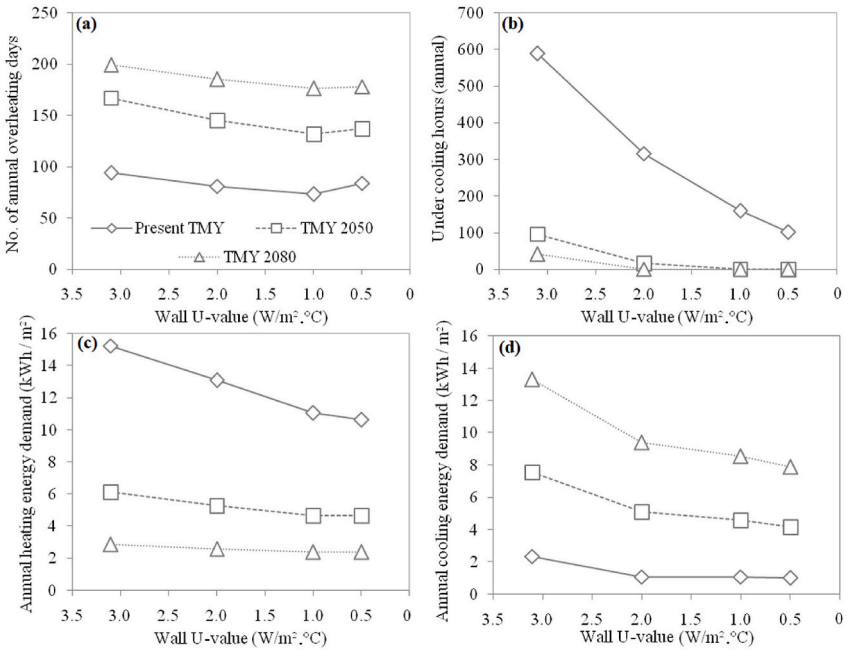

Fig. 17. Variation of (a) CIBSE overheating (days per year); (b) Indoor under cooling hours (hours per year); (c) heating demand; and (d) cooling demand with different wall U-values under different climatic scenarios. (Note: The decreasing U-values above represent the increasing thermal insulation).

Regarding the energy required for conditioning the building, there was a decrease in both the heating and cooling demand with a decrease in wall U-value (Fig. 17 (c) and (d)). To be more precise, a decrease in annual electrical energy demand by almost 30.2%, 24.0% and 17.4% for heating and 57.1%, 44.7% and 40.5% for cooling was noticed when the wall U-value decreased from 3.1 to 0.5 $W/m^2.^\circ C$ for the climatic scenarios of the present TMY, 2050 and 2080, respectively. Thus, it is an attractive proposal to consider insulations in wall envelope in newer buildings. A previous study predicted a decrease in cooling energy demand by 137% and 19.5%, and a decrease in heating energy demand by 24% and 8.0% when the wall U-value decreased from 5.0 to 0.20 $W/m^2.^\circ C$ for the climatic scenario of 2050 compared to the present in Venice [57].

4.4.3. Infiltration rate

With the decrease in air infiltration rate from 5 ACH (air change per hour) to 2 ACH, the annual overheating days decreased by 12.8%, 15.0% and 6.0%, the annual under-cooling hours decreased by 9.3%, 33.3% and 43.9%, the annual heating energy demand decreased by 2.5%, 3.0% and 3.2%, while the annual cooling energy demand decreased by 6.8%, 4.3% and 3.9% during the present TMY, 2050 and 2080 climatic scenarios, respectively. Hamdy et al. [26] earlier predicted that a high ventilation rate of over 5 ACH, reduced the overheating hours by 90% in Dutch buildings in the present climatic scenario. However, the indoor environmental quality was not studied in the present research which is largely affected by the ACH.

4.4.4. Window-to-wall ratio

The increase in the window-to-wall ratio had an increasing impact on the annual overheating days, while it had a decreasing impact on the annual under-cooling hours as seen in Fig. 18 (a) and (b). With the increase in window fraction, there is an increase in the solar gain which is responsible for this observation.

While there was a very small decrease in the requirement of annual heating energy demand, i.e., 0.4%, 0.4% and 0.3%, there was a substantial increase in the annual cooling energy demand, i.e., 33.0%, 16.1% and 9.6% with an increase in window-to-wall ratio from 30% to 80% during the climatic scenarios of present TMY, 2050 and 2080, respectively (Fig. 18 (c) and (d)). The increase in the solar gain during the daytime due to the increased window size could not decrease the heating energy required especially during the night time. However, the share of windows not only influences thermal comfort but also lighting issues. Aslanoglu et al. [61] stated that the satisfaction with daylight quality depends upon the factors that of daylight sufficiency, daylight uniformity, number of sunlight hours (i.e., the exposure to sunlight) and ratio of windows to the wall.

5. Discussion

A whole building performance of a multi-family, concrete 3-storey building built on the west-facing hill slope in Darjeeling Hills was performed using DesignBuilder V 6.0, which uses EnergyPlus simulation engine. The effects due to global warming of the mid and distant future climatic scenarios of 2050 and 2080 were analyzed using the CIBSE criteria 1–3 [25 and 46].

An increasing trend in the indoor operative temperature was noticed in all the zones in the future climatic condition of the year 2050 and 2080 compared to the present condition (Fig. 9). The percentage of time for which the indoor operative temperature was below 20 °C decreased in the future while that above 27 °C increased. However, it was noticed that the overheating in the top roof-exposed floor would deteriorate (a larger percentage of time the T_{op} was found to be over 27 °C), whereas the under-cooling inside the mid-floors would ameliorate (a lesser percentage of time the T_{op} would be below 20 °C). Further, the period of time for which the indoor conditions were within the ASHRAE Standard 55 [2] comfortable zone was 26.7%, 28.0% and 21.0% for the present climate, 34.1%, 38.5% and 31.1% for the year 2050 and 33.8%, 39.8% and 35.0% for the year 2080 in the top, middle and ground floor, respectively. This illustrates that with the increasing trend in the T_{op} during the future years, the number of comfortable indoor period increases on all the floors. This is due to the present under-cooled condition of the unheated house in the region. Also, it is understood that although during the present climate, due to cold condition the top floor having an exposed roof that receives a higher solar flux is more comfortable than the ground floor, this will not be the case during the climate-changed scenario of TMY 2080, when the mid floor exhibit a greater number of comfortable hours compared to the top floor. However, the increased indoor temperature (above 25 °C) along with a high RH (over 50%) can cause an increasing discomfort (except on the top floor) in the future years, i.e., 27.7%, 29.8% and 29.2% in the present climate, 21.2%, 35.2% and 37.7% in the year 2050 and 15.0%, 35.8% and 42.3% in 2080 in the top, middle and ground floor, respectively.

Similar differences in the indoor conditions were seen between the different parts, i.e., north, mid and south. It is clear that with global warming the northern part of the building will have a lesser number of hours below 20 °C, whereas the southern section of the building will have an increasing number of hours above 27 °C. The period for which the indoor condition is within the ASHRAE Standard 55 [2] comfort band is 29.1%, 25.2% and 13.3% during the present scenario, 34.6%, 36.0% and 23.1% during the 2050 condition and 32.5%, 38.3% and 27.6% during the 2080 climatic conditions inside the south, middle and north part of the building, respectively. Thus, with the increasing ambient temperature causing a lesser number of indoor under-cooled hours in this unheated building, the period for which the indoor conditions fall within the comfortable range inside the southern section of the building reaches a maximum in 2050 and decreases thereafter, whereas that in the mid and the north section keeps improving even after 2050. Due to the higher comfortable condition at present in the southern section of the building it was noticed to have a higher occupancy than the northern part, i.e. the occupants preferred to stay in this part of the building for most of the day. This is noticed from the higher occupancy in bedroom 2 (situated on the south) than in bedroom 1 (situated on the north) in Table 2, respectively. This also illustrates that although at present the southern part of the building which receives more sunlight is warmer and has a lesser frequency of under-heated indoor conditions making it the most comfortable part of the building, in the future due to overheating in this part, the middle part of the building will experience greater comfort.

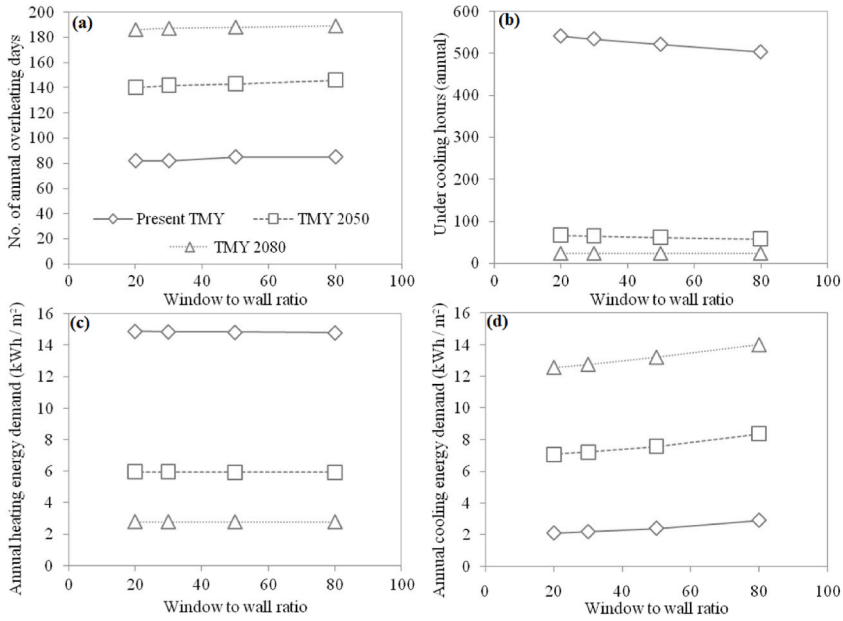

Fig. 18. Variation of (a) CIBSE overheating (days per year); (b) Indoor under cooling hours (hours per year); (c) heating demand; and (d) cooling demand with different window-to-wall ratio under different climatic scenarios.

Though the building currently runs on free-running mode, analysis for cooling and heating energy demand, normalized to floor area using grid-connected electricity was performed using the validated model. Fig. 13 shows the floor-wise energy demands for heating and cooling in the present and future climatic scenarios. The higher heating energy demand seen on the ground floor is due to the fact that it is more connected to the cool ground below. Secondly, lesser solar flux is received on the ground floor as the entire eastern and northern side of the building is blocked off from sunlight. Similarly, the higher cooling energy demand on the top floor is due to its greater exposure to solar radiation.

Fig. 14 illustrates the vertical section-wise energy demands for heating and cooling in the present and future climatic scenarios. As expected, the maximum energy demands for heating were seen in the northern part of the building, while overwhelmingly higher energy demands for cooling were noticed in the southern part of the building, in all the climatic conditions. This is due to a lesser solar flux received in the northern façade in comparison to that on the southern façade.

In addition, sensitivity analysis of the model was performed using the parametric differences in orientation, wall U-value, infiltration rate and window-to-wall ratio (Fig. 15-18). In a rugged hilly location, the major source of obstruction of solar radiation is the landscape. The investigated building which faces due west having its longer axis along the north-south direction performs the worst and is in the orientation having the highest overheating days and the highest cooling energy demand.

There were, however, some limitations in the present study. First, the calibration of the model for one year is done using on-site measurement of the indoor environment for only 10 days. Though from previous studies in the region, it was found that the day–night variations were more prominent than the seasonal changes, a measurement for indoor environmental, thermal and visual parameters for a longer duration would lead to a more robust model. Secondly, the present study focuses on a single building in the location. Though, the built form chosen was representative of the construction in the region, a future study with different typologies using statistical information from the building stock database for the area (or similar area) in order to make specific proposals that could be addressed for the rehabilitation of buildings in the area would be more interesting. Thirdly, the future climatic scenarios were based on the A2 scenario of the IPCC, which predicts a higher carbon-dioxide emission by the end of the 21st century along with fast and continued population growth and slow economic and technological development. However, the updated emission scenarios as per the Fifth IPCC report (AR5) would be more reliable in any future study. Finally, the study was conducted in the cold climate region found in Ref. [33] in northeast India, which experiences higher rainfall over snowfall. The emission scenario set was the A2 of the IPCC. Thus, the impact of the study on other climatic conditions across India [33], i.e., hot and dry, warm and humid, composite, temperate and cold climate found in the western Himalayas, which experiences lesser rainfall, needs to be studied. Further, the results need to be compared with that in the other emission scenarios of IPCC, i.e., A1, B1 and B2 [45]. The authors have kept this as a future scope of the model.

6. Conclusion

The IPCC predicts an inevitable warming in ambient temperature due to climate change and urges for a drastic reduction in the emission of global CO_2 by as much as 50% by 2030 and net zero by 2050, respectively. The indoor environment of presently built buildings that are free running is found prone to overheating even in the sub-Himalayan region of eastern India, which presently

experiences a cold climate.

A whole building simulation for indoor operative temperature, relative humidity and energy demand (electrical) for possible heating and air conditioning in view of climatic change during the present TMY, TMY 2050 and TMY 2080 was conducted for an existing 3-storey multifamily naturally ventilated building using the EnergyPlus in DesignBuilder. The established methodologies of hours of exceedance, daily weighted exceedance and upper limit temperature as prescribed by the CIBSE TM 52 were used to evaluate the indoor overheating. In addition, a methodology for the evaluation of indoor under-cooling was also presented.

An increasing trend in the indoor operative temperature during the future climatic condition was observed, with the top roof-exposed floor and the southern part of the building deteriorating the most. Though at present the southern part of this under-heated building was the most comfortable, the mid-level floors and the northern part of the building would benefit the most from the warming phenomenon and would become more comfortable to live in the future.

The parametric study showed that the existing west-facing building performed the worst in the event of global warming. The annual cooling demands were the lowest in the south-facing orientations, which would serve as a design guideline for the buildings that will be constructed in the region. Four different wall designs were considered, (i) existing single fire clay brick with plaster on both sides (U 3.1 $W/m^2.^\circ C$), (ii) double layer of fire clay brick (U 2.0 $W/m^2.^\circ C$), (iii) single AAC brick (U 1.0 $W/m^2.^\circ C$) and (iv) double AAC brick (U 0.5 $W/m^2.^\circ C$). It was observed that the overheating first decreased till the value of U reached 1.0 $W/m^2.^\circ C$. A further decrease in wall U-value led to an increase in indoor overheating. This is explained by the fact that at a low U-value, proper dissipation of indoor heat does not take place which causes indoor overheating. The study also showed that with the decrease in the air infiltration rate from 5 to 2 ACH, both the annual overheating days and annual under-cooling hours decreased in all the climatic conditions of the present, 2050 and 2080, respectively. However, the quality of indoor air needs to be considered while decreasing the air change rate, which was beyond the scope of the present study. Similarly, the decrease in the window-to-wall ratio also had a decreasing impact on the annual overheating days, while an increasing impact on the annual under-cooling hours and vice-versa. However, any decrease in the window-to-wall ratio needs to be compensated by its effect on daylight and visual comfort.

The present study which is conducted for the first time for a building located in the Himalayan region and which presently faces a cold climate revealed that the buildings in the region are prone to overheating of the indoor environment due to the global warming phenomenon. The study also revealed that the buildings that are oriented towards east/south-east direction would perform the best with regard to overheating in the face of climate change. The replacement of the conventional brick design with a single layer of AAC bricks is recommended. However, the U-values in the present study were taken for dry conditions. The region being one of the most humid, the infiltration of moisture in the envelope and the change in performance need to be first studied. Lastly, with the decrease in the infiltration rate and the decrease in the window-to-wall ratio, the thermal performance of the building was found to improve. However, these factors also affect the environmental (CO_2 build-up) and visual performance of indoors which were not considered in the present study.

With the increase in the economic status giving rise to a desire for improved indoor conditions, there is a huge potential that the use of air conditioning would increase in the future. This will cause a hike in emissions and thereby accelerate global warming. Thus a timely intervention, in how buildings are built in the developing world is of utmost essential as the huge population could be a severe threat to global warming. The parametric evaluation of wall U-values, orientation, ventilation rate and window-to-wall ratios as discussed in the paper will enable designers or architects in the region or in regions elsewhere with similar geo-climatic set up to evaluate trade-offs between these different factors and construct buildings that are more resilient in the face of climate change. Further, the discussion on the changes in floor-wise and section-wise performance of the building could enable the planners to plan the activities of the building adhering to thermal comfort and energy conservation opportunities.

Authors' contribution

Samar Thapa was responsible for overall research planning, design of experiment, data acquisition, analysis and manuscript preparation. Hom Bahadur Rijal, Wilmer Pasut and Ramkishore Singh provided supervision to the research. Madhavi Indraganti provided supervision in the manuscript draft. Ajay Kumar Bansal and Goutam Kumar Panda provided support in the research and manuscript preparation.

Declaration of competing interest

The authors declare that they have no known competing financial interests or personal relationships that could have appeared to influence the work reported in this paper.

Data availability

Data will be made available on request.

References

[1] F. Nicol, M. Humphreys, S. Roaf, Adaptive Thermal Comfort, Principles and Practice, first ed., Routledge, 2012, p. 8.
[2] ANSI/ASHRAE Standard 55 – 2020, Thermal Environmental Conditions for Human Occupancy, American Society of Heating, Refrigerating and Air Conditioning Engineers, Atlanta, GA, 2020.
[3] R.A. Martin, C.C. Federspiel, D.M. Auslander, Responding to thermal sensation complaints in buildings, Build. Eng. 108 (2002) 407–413.
[4] P.O. Fanger, Thermal Comfort Analysis and Applications in Environmental Engineering, McGraw Hill, New York, 1972.

[5] R.J. de Dear, G.S. Brager, Thermal comfort in naturally ventilated buildings: revisions to ASHRAE Standard 55, Energy Build. 34 (6) (2002) 563–572.
[6] BEE, Energy Conservation Building Code, Bureau of Energy Efficiency, 2007.
[7] Intergovernmental Panel on Climate Change (IPCC), Climate Change: the Physical Science Basis, 2021.
[8] P. Haves, G. Kenny, S. Roaf, The Impact of Climate Change on Buildings, Conference of Proc Passive and Low Energy Architecture, Auckland, 1992.
[9] S. Roaf, D. Crichton, F. Nicol, Adapting Buildings and Cities for Climate Change: A 21st Century Survival Guide, first ed., Elsevier, 2005, p. 2.
[10] J. Luterbacher, D. Dietrich, E. Xoplaki, M. Grosjean, H. Wanner, Europea seasonal and annual temperature variability, trends and extremes since 1500, Science 303 (2004) 1499–1503.
[11] K. Hayhoe, C. Cayan, C.B. Field, Emissions pathways, climate change and impacts on California, Proc. Natl. Acad. Sci. USA 101 (2004) 12422–12427.
[12] C. Mora, B. Dousset, I.R. Caldwell, F.E. Powell, R.C. Geronimo, C.R. Bielecki, C.W.W. Counsell, B.S. Dietrich, E.T. Johnston, L.V. Louis, M.P. Lucas, M. M. McKenzie, A.G. Shea, H. Tseng, T.W. Giambelluca, L.R. Leon, E. Hawkins, C. Trauernicht, Global risk of deadly heat, Nat. Clim. Change 7 (2017) 501, https://doi.org/10.1038/nclimate3322, 206.
[13] M. Baccini, A. Biggeri, G. Accetta, T. Kosatsky, K. Katsouyanni, A. Analistis, H.R. Anderson, L. Bisanti, D. D'lppoliti, J. Danova, B. Forsberg, S. Medina, A. Paldy, D. Rabczenko, C. Schindler, P. Michelozzi, Heat effects on mortality in 15 European cities, Epidemiology 15 (5) (2018) 711–719, https://doi.org/10.1097/ede.0b013e318176bfcd.
[14] A.K. Gupta, S. Guleria, Heat Wave 2016: A Documentation Study Based on the State of Telangana an Odisha States, 2018, https://doi.org/10.13140/RG.2.2.13035.23847.
[15] S. Thapa, Comfort zone calculation and climatic condition for a typical building located in the darjeeling hills, Salesian Journal of Humanities and Social Science II (2) (2011) 123–133. ISSN 0976 – 1861.
[16] IndiaSpend, 2019. Assessed 10 September, 2022. DOI: 65% Indians Exposed To Heatwaves In May-June 2019. July 2019 Was India's Hottest Ever (indiaspend.com).
[17] O. Verma, in: A.K. Taloor, B.S. Kotlia, K. Kumar (Eds.), Climate Change and its Impact with Special Reference to India, Water, Cyrosphere and Climate Change in the Himalayas, Springer – Geography of Physical Environment, 2021, pp. 39–55, https://doi.org/10.1007/978-3-030-67932-3_3.
[18] NIC Report, India: the Impact of Climate Change to 2030, National Intelligence Council, 2009, pp. 1–49. No. 03D, https://www.dni.gov/files/documents/climate2030_india.pdf.
[19] Gbpn, Building Policies for a Better World, Global Buildings Performance Network, 2021. https://www.gbpn.org/activities/india. (Accessed 6 August 2022). Accessed.
[20] R. Khosla, K.B. Janda, India's building stock: towards energy and climate change solutions, Build. Res. Inf. 47 (2019) 1–7.
[21] D.H.W. Li, L. Yang, J.C. Lam, Impact of climate change on energy use in the built environment in different climate zones – a review, Appl. Energy 42 (1) (2012) 103–112.
[22] Y. Yang, K. Javanroodi, V.M. Nik, Climate change and energy performance of European residential building stocks – a comprehensive impact assessment using climate big data from the coordinated regional climate downscaling experiment, Appl. Energy 298 (117246) 1–23, 2021.
[23] M. Santamouris, Cooling of buildings, Past, Present and Future, Energy and Buildings 128 (2016) 617–638, 2016.
[24] M. Santamouris, On the energy impact of urban heat island and global warming on buildings, Energy Build. 82 (2014) 100–113, 2014.
[25] CIBSE, Environmental Design CIBSE Guide A, seventh ed., Chartered Institution of Building Services Engineers, London, 2006.
[26] M. Hamdy, S. Carlucci, P.J. Hoes, J.L.M. Hensen, The impact of climate change on the overheating risk in dwellings – a Dutch case study, Build. Environ. 122 (2017) 307–323.
[27] R. Rahif, M. Hamdy, S. Homaei, C. Zhang, P. Holzer, A. Attia, Simulation-based framework to evaluate resistivity of cooling strategies in buildings against overheating impact of climate change, Build. Environ. 208 (2022) (2022) 1–18, 108599.
[28] J. Zou, A. Gaur, L. Wang, A. Laouadi, M. Lacasse, Assessment of future overheating conditions in Canadian cities using a reference year selection method, Build. Environ. 218 (2022) (2022) 1–21, 109102.
[29] S. Kumar, Subject's thermal adaptation in different built environments: an analysis of updated metadata-base of thermal comfort data in India, J. Build. Eng. 46 (2022), 103844.
[30] S. Thapa, Thermal comfort in high altitude himalayan residential houses in darjeeling, India – an adaptive approach, Indoor Built Environ. 29 (1) (2019) 88–100.
[31] M.K. Singh, S. Mahapatra, S.K. Atreya, Study to enhance comfort status in naturally ventilated vernacular buildings of north-east India, in: Proceedings of the ISES Solar World Congress 2009, Renewable Energy Shaping our Future, 2009, pp. 1442–1450.
[32] K. Heena, A. Saifudeen, M. Mani, Resilience of vernacular and modernizing dwellings in three climatic zones to climate change, Sci. Rep. 11 (9172) (2001) 1–14.
[33] Indian Standard SP 7 – NBC, National Building Code (NBC) of India, BIS, New Delhi, 2016. Bureau of Indian Standards, 2016.
[34] BEE, Energy Conservation Building Code, Bureau of Energy Efficiency, 2007.
[35] L. Yang, H. Yan, Y. Xu, J.C. Lam, Residential thermal environment in cold climates at high altitude and building energy use implications, Energy Build. 62 (2013) 139–145.
[36] A.L. Escamilla, R.H. Limones, A.L.L. Rodriguez, Evaluation of environmental comfort in a social housing prototype with bioclimatic double-skin in a tropical climate, Build. Environ. 218 (2022) 1–15, 109119.
[37] 2021 S. Liu, T. Kwok, K. Lau, E. Ng, Applicability of different extreme weather datasets for assessing indoor overheating risks of residential buildings in a subtropical high-density city, Build. Environ. 194 (2021) 1–20, 107711.
[38] A. Dodoo, L. Gustavsson, F. Bonakdar, Effects of future climate change scenarios on overheating risk and primary energy use for Swedish residential buildings, Energy Proc. 61 (2014) 1179–1182, 2014.
[39] S. Liu, Y.T. Kowk, K. Ka-Lun Lau, W. Ouyang, Effectiveness of passive design strategies in responding to future climate change for residential buildings in hot and humid Hong Kong, Energy Build. 228 (110469) (2020) 1–13, 2020.
[40] B. Atanasiu, Principles for Nearly Zero Energy Buildings: Paving the Way for Effective Implementation of Policy Requirements, Buildings Performance Institute, Brussels, 2011. ISBN9789491143021.
[41] U. PMAY (, Pradhan Mantri Awas Yojna (Urban) – Ministry of Housing and Urban Affairs, Government of India, New Delhi, 2015. https://pmaymis.gov.in/.
[42] R. Escandon, R. Saurez, A. Alonso, G.M. Mauro, Is indoor overheating an upcoming risk in southern Spain social housing stocks? Predictive assessment under a climate change scenario, Build. Environ. 207 (2022) 1–10, 108482.
[43] A. Ioannou, L.C.M. Itard, Energy performance and comfort in residential buildings: sensitivity for building parameters and occupancy, Energy Build. 92 (2015) 216–233.
[44] M. Hosseini, K. Javanroodi, V.M. Nik, High-resolution impact assessment of climate change on building energy performance considering extreme weather events and microclimate – investigating variations in indoor thermal comfort and degree days, Sustain. Cities Soc. 78 (103634) (2022) 1–21.
[45] Intergovernmental Panel on climate change, World Meteorological Organization (2000), Summary for Policymakers, IPCC Special Report on Emissions Scenarios, A Special Report of IPCC Working Group III, ISBN: 92-9169-113-5, vol 1, pp 1 - 27.
[46] T.M.52 CIBSE, The Limits of Thermal Comfort: Avoiding Overheating in European Buildings, Chartered Institution of Building Services Engineers, London, 2013.
[47] E.N. CEN, Indoor Environmental Input Parameters for Design and Assessment of Energy Performance of Buildings Addressing Indoor Air Quality, Thermal Environment, Lighting and Acoustics, Comitee European de Normalisation (CEN), Brussels, 2007, 15251, 2007.
[48] E.N. CEN, Energy Performance of Buildings – Ventilation for Buildings –Part 1: Indoor Environmental Input Parameters for Design and Assessment of Energy Performance of Buildings Addressing Indoor Air Quality, Thermal Environment, Lighting and Acoustics – Module M 1 – 6, Comitee European de Normalisation (CEN), Brussels, 2020, 16798.
[49] CIBSE, Design Methodology for the Assessment of Overheating Risk in Homes, in: Technical Memorandum TM, 59, Chartered Institution of Building Services Engineers, London, 2017.

[50] IPCC, Intergovernmental Panel on climate change, Global Warming of 1.5 °C. An IPCC Special Report on the impacts of global warming of 1.5 °C above pre-industrial levels and related global greenhouse gas emission pathways, in the context of strengthening the global response to the threat of climate change, sustainable development, and efforts to eradicate, poverty, Summary for Policymakers, 2018, 2018, ISBN 978-92-9169-151-7, vol 1, pp 1 - 32.
[51] S. Thapa, A.K. Bansal, G.K. Panda, Adaptive thermal comfort in the residential buildings of north east India – an effect of difference in elevation, Build. Simulat. 11 (2) (2018) 245–267, https://doi.org/10.1007/s12273-017-0404-x.
[52] WHO, WHO Housing and Health Guidelines, World Health Organization, Switzerland, 2018.
[53] M. Bhatnagar, J. Mathur, V. Garg, Determining base temperature for heating and cooling degree days for India, J. Build. Eng. 18 (2018) 270–280.
[54] S. Thapa, Risk of overheating in low-rise naturally ventilated residential buildings of northeast India – an effect of climate change, Architect. Sci. Rev. (2021), vol 65, issue 1, 2022, pp 14 - 41.
[55] S. Thapa, Investigation of Thermal Comfort and Adaptation Among the Residents of Cold Climate in the Lower Himalayan Region of Eastern India, Indoor and Built Environment, 2022, vol. 31, issue 6, pp. 1613 - 1635.
[56] I.G. Dino, C.M. Akgul, Impact of climate change on the existing residential building stock in Turkey: an Analysis on Energy use, greenhouse gas emissions and occupant comfort, Renew. Energy 141 (2019) 828–846.
[57] E. Rodrigues, M.S. Fernandes, Overheating risk in mediterranean residential buildings: comparison of current and future climate scenarios, Appl. Energy 259 (2019) 1–12.
[58] ASHRAE Guideline, Measurement of Energy, Demand and Water Savings, 14, 2014. www.ashrae.org.
[59] S. Thapa, A.K. Bansal, G.K. Panda, M. Indraganti, Adaptive thermal comfort in the different buildings of Darjeeling Hills in eastern India – effect of difference in elevation, Energy Build. 173 (2018) 649–677.
[60] M. Cellura, F. Guarino, S. Longo, Tumminia, Climate change and the building sector: modelling and energy implications to an office building in southern Europe, Energy for Sustainable Development 45 (2018) 46–65.
[61] 2021 R. Aslanoglu, J.K. Kazak, S. Yekanialibeiglou, P. Pracki, B. Ulusoy, An international survey on residential lighting: analysis of winter-term results, Build. Environ. 206 (2021) 1–12, 108294.